

Optimizing The DSSC Fabrication Process Using Lean Six Sigma

by

Brian Fauss

A Thesis Presented in Partial Fulfillment
of the Requirements for the Degree
Master of Science in Technology

Approved November 2012 by the
Graduate Supervisory Committee:

Lakshmi Munukutla, Chair
Arunachalanadar Madakannan
Gerald Polesky

ARIZONA STATE UNIVERSITY

December 2012

ABSTRACT

Alternative energy technologies must become more cost effective to achieve grid parity with fossil fuels. Dye sensitized solar cells (DSSCs) are an innovative third generation photovoltaic technology, which is demonstrating tremendous potential to become a revolutionary technology due to recent breakthroughs in cost of fabrication. The study here focused on quality improvement measures undertaken to improve fabrication of DSSCs and enhance process efficiency and effectiveness. Several quality improvement methods were implemented to optimize the seven step individual DSSC fabrication processes. Lean Manufacturing's 5S method successfully increased efficiency in all of the processes. Six Sigma's DMAIC methodology was used to identify and eliminate each of the root causes of defects in the critical titanium dioxide deposition process. These optimizations resulted with the following significant improvements in the production process: 1. fabrication time of the DSSCs was reduced by 54 %; 2. fabrication procedures were improved to the extent that all critical defects in the process were eliminated; 3. the quantity of functioning DSSCs fabricated was increased from 17 % to 90 %.

ACKNOWLEDGMENTS

First and foremost, a sincere thank you to Dr. Lakshmi Munukutla, my committee chair, for exceptional guidance and support throughout the project, undergraduate and graduate program. Dr. Munukutla's caring nature, professional advice, and words of encouragement gave me confidence to pursue the Master's Degree in Alternative Energy at ASU.

Dr. Gerald Polesky also deserves a large amount of credit for the success of this project through his continuous mentorship in Lean Six Sigma, as well as his undeniable dedication to all of his students.

I am also grateful for the assistance, support and advice that I have received from so many professors, colleagues and businesses. Dr. Arunachalanadar Madakannan, Dr. Govindasamy Tamizhmani, and Dr. Bradley Rogers professional advice and constructive criticism helped strengthen the foundation of my project. Thank you Laura Main, Travis Curtis, Trian Georgeou, Rene Fischer, Martha Benton, and Julie Barnes for your assistance with the fabrication and background support throughout this project. Assistance received from Tara Fauss and Applied Plastics Machining, Terry Stringer of Ellsworth Adhesives, and Auburn Manufacturing Company were all greatly appreciated.

My parents, Dave and Ann Fauss deserve special recognition for teaching me the value of continuing education through leading by example. Their help in revisions and critiques formed this thesis into a professional document that I will always cherish.

Lastly, I would like to give a special thanks to my wonderful wife for her endless patience, love and support, and help raising our two young children. Karina selflessly placed her career on hold to allow me the opportunity to complete this research and graduate degree.

TABLE OF CONTENTS

	Page
LIST OF TABLES	x
LIST OF FIGURES	xii
CHAPTER	
1 INTRODUCTION	1
1.1 Purpose	1
1.2 Background	3
1.3 Scope.....	6
2 LITERATURE REVIEW	8
2.1 Solar Technology.....	8
2.1.1 Motivation for Solar Technologies	8
2.1.2 Solar Technology Types	9
2.1.2.1 History	9
2.1.2.2 Crystalline Silicon Solar Cells.....	10
2.1.2.3 Thin Film Solar Cells	11
2.1.2.4 Third-Generation Solar Technologies	11
2.2 The Dye-Sensitized Solar Cell	14
2.2.1 DSSC History.....	14
2.2.2 Fundamental Operation	15
2.2.3 Structure.....	17
2.2.3.1 Glass Electrodes	18

CHAPTER	Page
2.2.3.2 Counter Electrodes.....	19
2.2.3.3 Working Electrodes	19
2.2.3.4 Dye Sensitizer	20
2.2.3.5 Sealant	21
2.2.3.6 Electrolyte.....	22
2.2.4 Solar Cell Parameters.....	22
2.3 Lean Six Sigma	25
2.3.1 Summary of LSS.....	25
2.3.2 Lean Manufacturing	25
2.3.3 Six Sigma.....	26
2.4 Standard Operating Procedures.....	28
3 EXPERIMENTAL METHODS	30
3.1 Fabrication Improvements.....	30
3.1.1 Titanium Dioxide Deposition Process.....	31
3.1.1.1 TiO ₂ Deposition Problem Statement.....	31
3.1.1.2 Original Procedure	32
3.1.1.3 Steps Taken to Improve Methodology	34
3.1.1.3.1 Define Phase at Benchmark #1	36
3.1.1.3.2 Measure Phase.....	36
3.1.1.3.3 Analyze Phase.....	40
3.1.1.3.4 Improve Phase.....	41

CHAPTER	Page
3.1.1.3.5 Control Phase	42
3.1.1.3.6 Define Phase at Benchmark #2.....	43
3.1.1.3.7 Measure Phase.....	43
3.1.1.3.8 Analyze Phase.....	44
3.1.1.3.9 Improve Phase.....	45
3.1.1.3.10 Control Phase	46
3.1.1.3.11 Define Phase at Benchmark #3.....	47
3.1.1.3.12 Measure Phase.....	47
3.1.1.3.13 Analyze Phase	48
3.1.1.3.14 Improve Phase.....	49
3.1.1.3.15 Control Phase	50
3.1.1.3.16 Define Phase at Benchmark #4.....	51
3.1.1.3.17 Measure Phase.....	51
3.1.1.3.18 Analyze Phase	52
3.1.1.3.19 Improve Phase.....	53
3.1.1.3.20 Control Phase	55
3.1.2 Glass Cutting Process	56
3.1.2.1 Glass Cutting Problem Statement.....	57
3.1.2.2 Original Procedure	57
3.1.2.3 Steps Taken to Improve Methodology	58
3.1.2 Glass Drilling Sub-process	60

CHAPTER	Page
3.1.3.1 Glass Drilling Problem Statement	60
3.1.3.2 Original Procedure	60
3.1.3.3 Steps Taken to Improve Methodology	61
3.1.4 Platinum Deposition Process	63
3.1.4.1 Platinum Deposition Problem Statement	63
3.1.4.2 Original Procedure	63
3.1.4.3 Steps Taken to Improve Methodology	64
3.1.5 Dye Solution Preparation Sub-process	65
3.1.5.1 Dye Solution Prep. Problem Statement	66
3.1.5.2 Original Procedure	66
3.1.5.3 Steps Taken to Improve Methodology	66
3.1.6 Sealant Preparation Sub-process	67
3.1.6.1 Sealant Preparation Problem Statement	67
3.1.6.2 Original Procedure	67
3.1.6.3 Steps Taken to Improve Methodology	68
3.1.7 Final Cell Assembly Process	69
3.1.7.1 Final Cell Assembly Problem Statement	69
3.1.7.2 Original Procedure	70
3.1.7.3 Steps Taken to Improve Methodology	71
3.2 Project Improvements	75
3.2.1 Lean Manufacturing	75

CHAPTER	Page
3.2.2 Solar Testing Station.....	76
3.2.2.1 Solar Testing Station Problem Statement.....	77
3.2.2.2 Original Procedure	77
3.2.2.3 Steps Taken to Improve Methodology	78
4 RESULTS AND DISCUSSION	83
4.1 Fabrication Improvements.....	83
4.1.1 Titanium Dioxide Deposition	83
4.1.2 Dye Solution Preparation	86
4.1.3 Glass Cutting	87
4.1.4 Glass Drilling	88
4.1.5 Platinum Deposition	89
4.1.6 Sealant Preparation	90
4.1.7 Final Assembly.....	91
4.2 Project Improvements	92
4.2.1 Lean Manufacturing	92
4.2.1 Solar Testing Station.....	94
4.3 Combined Results	95
5 CONCLUSION	97
5.1 Overview.....	97
5.2 Future Recommendations	99
REFERENCES	101

APPENDIX

Page

A STANDARD OPERATING PROCEDURE (SOP) 110

LIST OF TABLES

Table		Page
3.1.	DMAIC tools used to improve the TiO ₂ process	35
3.2.	Checklist of defects during the initial process	37
3.3.	Checklist of defects at Benchmark #2	44
3.4.	Checklist of defects at Benchmark #3	48
3.5.	Checklist of defects at Benchmark #4	51
3.6.	Checklist of defects at Benchmark #5	55
4.1.	Titanium Dioxide Deposition Process Sigma	85
4.2.	Titanium dioxide deposition improvements in process and procedure times	86
4.3.	Improvement in dye solution preparation time	87
4.4.	Improvements in glass cutting procedure time and success rate	88
4.5.	Improvements in glass drilling procedure time and success rate	89
4.6.	Improvement in platinum deposition process and procedure times	90
4.7.	Sealant preparation improvement in preparation time	91
4.8.	Improvements in final assembly process and procedure times	92

Table		Page
4.9.	Comparison of time to test original and modified process on three cells, three times per week	94
5.1.	Percent improvement of procedural times and percent reduction of defects with each process	98

LIST OF FIGURES

Figure		Page
2.1.	Best Research-Cell Efficiencies	12
2.2.	Energetic Schematic of a DSC	16
2.3.	Layered components of a DSSC	18
2.4.	Chemical Structure of Ruthenium N719 dye	21
2.5.	I-V Curve Characterization	23
2.6.	The influence of shunt and series resistance	24
3.1.	DSSC fabrication improvement flow chart	30
3.2.	Coating TiO ₂ using a glass rod	33
3.3.	TiO ₂ coating methods using a steel doctor blade	33
3.4.	Original TiO ₂ Deposition Process Map	36
3.5.	Microscope and monitor used to view TiO ₂ defects	37
3.6.	Sintered TiO ₂ defects	38
3.7.	TiO ₂ flaking	38
3.8.	Pareto Chart of initial TiO ₂ deposition process	39
3.9.	The Cause-and-Effect Diagram for TiO ₂ Dep. Defects	40
3.10.	U Chart prior to the first improvement	41
3.11.	U Chart after the first set of improvements	42
3.12.	TiO ₂ layers following the first set of improvements	42
3.13.	Process Map following the first set of improvements	43
3.14.	Pareto Chart at Benchmark #2	44

Figure	Page
3.15. The Cause-and-Effect Diagram at Benchmark #2	45
3.16. U Chart after the second set of improvements	46
3.17. TiO ₂ layers following the second set of improvements	46
3.18. Process Map following the second set of improvements	47
3.19. Pareto Chart at Benchmark #3	47
3.20. The Cause-and-Effect Diagram at Benchmark #3	48
3.21. U Chart after the third set of improvements	49
3.22. TiO ₂ layers following the third set of improvements	50
3.23. Process Map following the third set of improvements	51
3.24. Pareto Chart at Benchmark #4	52
3.25. The Cause-and-Effect Diagram at Benchmark #4	53
3.26. TiO ₂ hand coating method	54
3.27. A hand coated TiO ₂ layer after sintering	54
3.28. TiO ₂ layers following the fourth set of improvements	55
3.29. Process Map following the fourth set of improvements	56
3.30. Drilling setup	62
3.31. Coating Platisol on electrodes	65
3.32. Sealant cutting procedure	69
3.33. Original solar cell assembly technique	71
3.34. DSSC assembly presses	72
3.35. SolidWorks® 2012 drawings of assembly presses	73

Figure	Page
3.36. DSSC presses in use	74
3.37. Mounted testing station	80
3.38. Photograph of testing jig on platform	81
3.39. Testing platform setup	82
4.1. Effect of DMAIC on defects during TiO ₂ deposition	84
4.2. Optimized DSSC fabrication flow chart	93
4.3. Amount of time required to complete procedures	96

Chapter 1

INTRODUCTION

1.1 Purpose

The research focus is to analyze the effectiveness of the dye-sensitized solar cells (DSCCs) fabrication process control at Arizona State University's (ASU's) Polytechnic Campus. Several factors were considered, which led to the adoption of this study. Many graduate students spend an overwhelming amount of time learning what past researchers have already done rather than concentrating on their topic. However, this study served as impetus for this research. The goal of this experiment is to implement process control methods to achieve repeatable fabrication process that yields consistent results so that future researchers can optimize their time on individual research topics. Systematic process improvements will be implemented by taking an analytical approach to solving the problems.

Since 2009, several research projects at ASU have focused on optimizing DSSC stability and performance. One previous researcher compared various electrolytes, while another studied characteristics of the titanium dioxide (TiO_2) layer to improve cell performance. The most recent researcher studied the effects of adding single-walled carbon nano-tubes (SWCNT) to the TiO_2 layer and sputtering platinum nanoparticles onto the

counter electrode [1]. These projects provided excellent studies on how to optimize individual key components of the DSSC.

Since its beginning, DSSC fabrication procedures have steadily evolved on this project. However, due to manual fabrication processes several non-standardization fabrication methods and procedures have prevented the consistent production of optimized DSSCs. A wide assortment of defects occurred throughout the entire fabrication process. Every defect negatively impacts cell performance, but certain defects are fatal, and as a result non-functional DSSCs are yielded.

Scientific experiments compare results against a known value. Inconsistent results from defective processes make it difficult to draw valid conclusions. This is precisely why reliable processes are essential to assure reproducible results in the laboratory.

Fabricating the DSSCs includes four processes and three supporting sub-processes. Various methods were used to improve and control the DSSC fabrication processes and procedures, but no single method suited every process. A list of methods used for controlling the DSSC fabrication processes included: fundamental principles of Lean manufacturing and Six Sigma (5S, DMAIC), thermal modeling, and standardization through “standard operating procedures” (SOPs).

1.2 Background

Tremendous advances in technology have improved the standard quality of life in most cultures worldwide. As a result, humanity has grown accustomed to rely heavily on electrical energy. Combine this increased demand for energy with a sharply rising human population, and the ingredients present for a rapidly approaching energy crisis. Generally, it is recognized that sole dependence on fossil fuels is not sustainable, and as a result, alternative energy technologies have been called upon as a solution to relieve the unsustainable energy demand on fossil fuel. Solar technology uses the most direct energy conversion process of all the technologies to produce electricity without creating carbon dioxide emissions or greenhouse effects [2]. Solar cells accomplish this by harnessing radiated energy from the sun. The sun is a massive energy source that will continue to radiate energy well beyond a billion years.

Solar technologies have evolved into three different generations of cells. Crystalline silicon and thin film are the second and third generations of solar technologies respectively. DSSCs fall among the third and most recent generation of innovative solar cells. The DSSC is a photochemical cell with a unique cost-effective design made with a variety of available materials. DSSC conversion efficiencies have exceeded 12 %, but problems such as containment of the volatile electrolyte, electron recombination, and difficulties with scalability suppress the

commercialization of the technology. Once these issues are resolved, DSSCs may be a more viable option.

Fabrication of the DSSC is simple in theory, but is deceptively sensitive to minor adjustments in nearly every aspect. Impacting variables include: changes in material composition and interactions, geometric variances, thermal cooling and heating rates, storage conditions, ambient temperatures, humidity, and foreign contaminants. Such variables are actively monitored in fully automated manufacturing facilities using precision equipment and environmental controls. However, this is generally not feasible in a research setting. Artisan type fabrication procedures are often performed to produce small batches of samples. Because of this, many opportunities for defects are introduced in a manual process that would not exist in an automated process.

Fortunately, process control methods are not only useful for industry manufacturing optimization, but may also be used to increase effectiveness and efficiency in nearly any process requiring precision and accuracy. Quality improvement methodologies were originally thought to be useful only in mass production environments, but have since proven valuable in many other fields including: health care [3-4], engineering [5], software [6], and research [7-8].

Lean Six Sigma (LSS) is a popular quality improvement methodology that is used by many of the most successful solar cell

production companies in the world. These companies have demonstrated the ability of using Lean Six Sigma to significantly reduce waste and defects while also reducing production costs and time. Those companies experienced long-term improvements in productivity and profitability despite the extra costs and effort of implementing LSS [9-10].

Many, if not most, large companies employ entire teams or departments to ensure quality process control and optimization. The same companies also follow strict protocols and standards, which are often included within “good manufacturing practices” (GMP). Likewise, research laboratories have their own set of quality practices and standards called “good laboratory practices” (GLP). Following these standards can be considered an optional luxury that not all laboratories can afford. The DSSC project at ASU is among those that cannot afford to commit resources to implement such standards. However, this experiment successfully implemented several quality control methods and standards to gain process control at a minimal cost.

Continually growing global competition has forced many companies to explore new innovative ideas to gain or maintain competitive advantage. Innovation revolves around change, and change frequently introduces new forms of unwanted variation. Variation in manufacturing and fabrication often results in defects and inconsistencies. Quality control methods such as Lean Six Sigma and standardization have played

important roles during these transitions to minimize defects and inconsistencies.

This experiment conducted at ASU will use appropriately scaled down quality control methods on the fabrication process of DSSCs. Results will then be reviewed and compared against results experienced by manufacturing companies to determine the scalability of the process control methods.

The following Chapter 2 will familiarize the reader with the history and background of solar technologies, DSSCs, and Lean Six Sigma. It is important to comprehend fundamental concepts related to the experiment prior to discussing the experimental methods in Chapter 3. Results of this study are discussed in Chapter 4.

1.3 Scope

This experiment will focus on improving five individual processes and three individual sub-processes as listed below.

- Titanium Dioxide Deposition – Fabrication Process
- Dye Solution Preparation – Fabrication Sub-process
- Glass Cutting – Fabrication Process
- Glass Drilling – Fabrication Sub-process
- Platinum Deposition – Fabrication Process
- Final Cell Assembly – Fabrication Process
- Sealant Preparation – Fabrication Sub-process

- Solar Testing Station – Project Process

DSSCs are first fabricated and then tested for performance. The items listed above are the individual processes and sub-processes that are performed to fabricate and test DSSCs. The fabrication processes will be modified for improvement in order to obtain proper control. The solar testing station will be modified to conform to testing standards.

The root causes of defects for the titanium dioxide deposition process could not be determined, therefore, Lean Manufacturing's 5S method and Six Sigma's DMAIC methodology was used to improve and control these processes.

The Solar Simulator Testing Process is used for measuring the performance of completed DSSCs. The process is not directly part of the overall DSSC fabrication process, but will be improved because of its importance for gauging progress. Variation, time, and defects will be used as data throughout the experiment. Cell efficiencies and performances will be observed but not included within the scope of this project.

Chapter 2

LITERATURE REVIEW

2.1 Solar Technology

2.1.1 Motivation for Solar Technologies

Fossil fuels continue to be the most prevalent supply of energy resources available. These include diesel, gasoline, coal and natural gas. However, human populations continue to sharply increase, driving up the demand for energy. Fossil fuel prices steadily increase as the supplies dwindle. To help relieve some of the growing demand, alternative energies are being sought and developed. Although it is not currently feasible to completely replace fossil fuels with alternative energy sources, alternative energy is expected to assume a larger share of the energy market in the future.

As worldwide power consumption increases, excessive amounts of carbon emissions continue to accumulate. Carbon monoxide and carbon dioxide harm biological species as well as the planet's ecology, such as temperatures and oceanic currents. Taking advantage of the abundant solar energy is one of the best ways of reducing the use of fossil fuels and therefore, driving down carbon emissions. Even though solar energy has a large potential to reduce emissions and provide substantial amounts of power to consumers, solar energy accounted for only 1.7 % of the total energy produced by alternative energy sources in 2011 [11].

Solar energy prices continue to drop, but have not yet achieved grid parity. Grid parity is critical for any alternative energy to be competitive to current energy-dominant fossil fuel energy sources. Solar technologies continue to evolve, but still have a long way to go to be competitive with fossil fuels and other alternative energy sources.

Even though solar energy represents only 1.7 % of the alternative energy market, it has grown 40 % annually over the last decade due to generous government subsidies [12]. The use of numerous other alternative energy technologies such as wind, geothermal, hydro and biofuels have grown at astonishing rates as well. Yet the solar energy technology possesses a key advantage over other technologies. It benefits from using the most widely abundant source of energy - photons from the sun. Photons are packets of light energy, which transmit from the sun at different frequencies. The sun is expected to shine for billions of years, well beyond the existence of Earth. Solar cells have semiconducting materials that absorb light energy and transform it directly into electricity.

2.1.2 Solar Technology Types

2.1.2.1 History

In 1839, Edmond Becquerel found that an electric potential exists between two electrodes attached to a solid or liquid system upon light irradiation [13]. This is known as the photovoltaic effect. The discovery of

the photovoltaic effect laid the foundation for many different solar converting technologies. Present day solar cells can be classified into two main types, crystalline silicon solar cells and thin film solar cells. These types fall into three generations of solar technologies.

2.1.2.2 Crystalline Silicon Solar Cells

Single (mono) crystalline and multi (poly) crystalline solar cells are made from silicon crystals, and are both first generation crystalline silicon solar cells. Crystalline solar modules presently dominate the solar market. As of November 2011, the average efficiencies of crystalline silicon (c-Si) solar modules have risen to 15.4 % [12]. SunPower Corporation has announced a limited production of modules, which convert energy at an amazing 24 % efficiency [12]. This highlights how close solar technologies are to reaching the theoretical efficiency limits; for c-Si solar cells the theoretical efficiency limit is 29 %.

Although efficiencies are improving and production costs continue to decrease, c-Si solar cells are still more costly than using competing fossil fuels. Improving performance efficiencies and production costs are making solar more attractive, however, c-Si solar cells are still manufactured using highly expensive and controversial wafer processes, which involve growing, polishing, slicing and applying chemical treatments. Polycrystalline (poly-Si) cells display low conversion

efficiencies of around 14 %, but are considerably cheaper to produce than c-Si cells.

2.1.2.3 Thin Film Solar Cells

Thin film solar cells are considered the second generation of solar cells. The thin film solar cell family includes: Amorphous, Copper Indium Gallium Diselenide (CIS or CIGS) and Cadmium Telluride (CdTe). Second generation solar cells were originally considered low-cost low-efficiency cells; however, these cells now possess the ability to be low-cost high-efficiency cells.

2.1.2.4 Third Generation Solar Technologies

The defining criteria for third generation solar cells are somewhat ambiguous. Technologies within this category of solar cell technology are still in the research phases. They are considered the third generation of solar cells.

Best Research-Cell Efficiencies

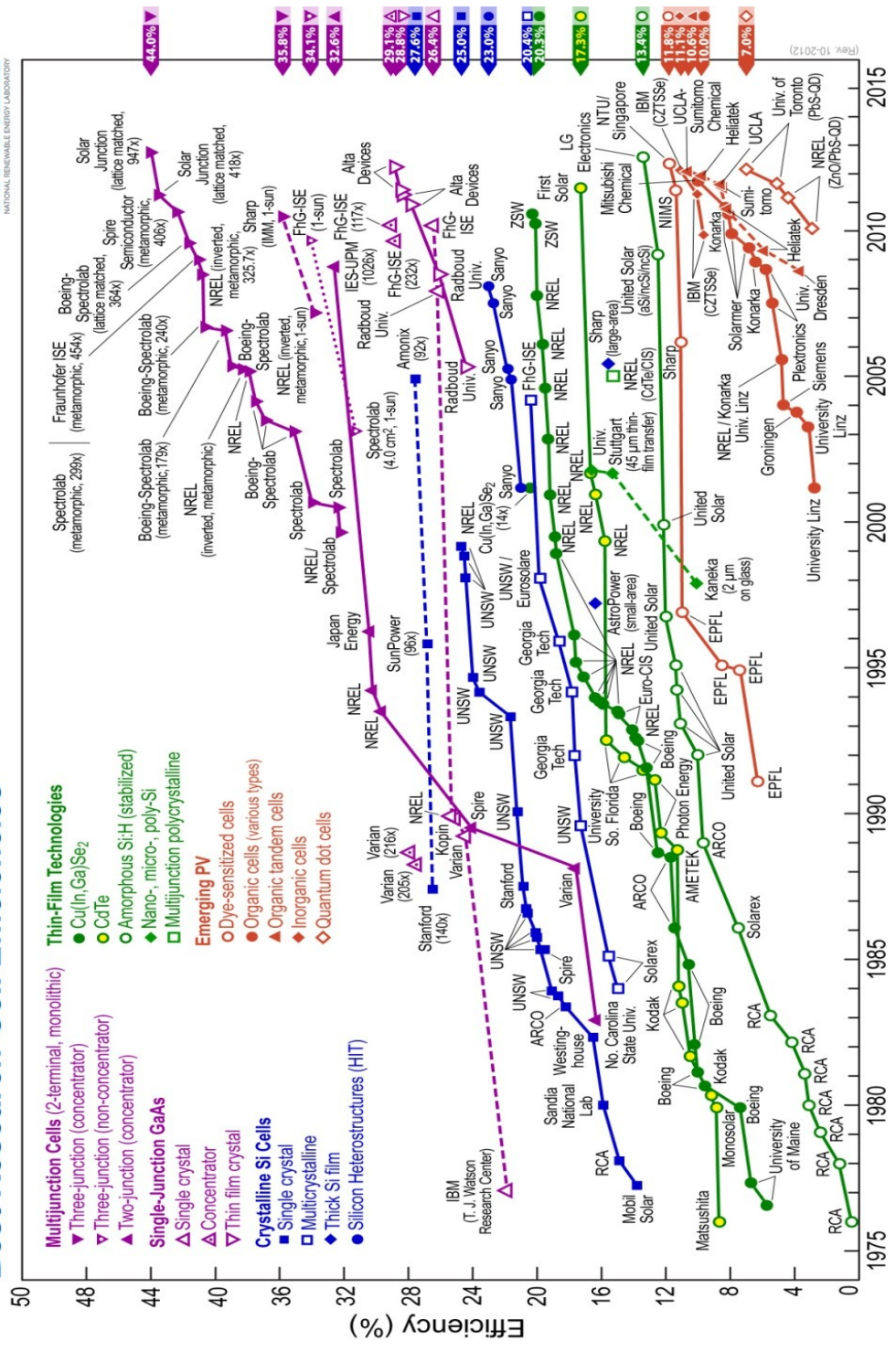


Figure 2.1: Best Research-Cell Efficiencies [14]

Figure 2.1 illustrates that third generation solar cell technologies (orange and purple text) continue to improve, whereas improvements on first and second generation solar technologies (blue and green text, respectively) have stagnated. Third generation solar cells are expected to combine the best qualities of the previous two generations of solar cells: low production costs, high performance efficiencies and appealing aesthetics.

Unlike silicon-based cells, third generation cells do not require a p-n junction to operate. Some of the many innovations included in third generation technologies include: polymer solar cells, biomimetics, intermediate band solar cells, tandem/multi-junction cells, hot-carrier cells, photon upconversion and downconversion technologies, solar thermal technologies, nanocrystalline solar cells, Quantum Dot Solar Cells (QDSCs), Dye-Sensitized Solar Cells (DSSCs), and organic solar cells.

Multi-junction concentrated solar cells have achieved the record high efficiencies of greater than 40 % at a cost of 0.14 \$/kWh [15]. Multi-junction solar modules have already penetrated the solar market.

DSSCs are another third generation solar technology that has been recently introduced into the consumer market [16-17]. DSSCs involve simple fabrication procedures and have promising applications on flexible substrates [18]. Since DSSC fabrication cost is lower than a silicon solar cell, this technology has the potential to be used in many applications.

However, there is still room to improve the performance of DSSCs in order to further enhance its potential before commercialization.

2.2 The Dye-Sensitized Solar Cell

2.2.1 DSSC History

Michael Grätzel and Brian O'Regan introduced the DSSC first in 1991 [19]. Grätzel and O'Regan's discovery was based on the original photovoltaic effect concept. The highest record of the solar conversion efficiency in DSSCs is around 12.3 % as reported in the literature [20]. Researchers continue improving solar conversion efficiencies by altering and optimizing DSSC components.

Using dyes to sensitize wide band gap semiconductors is not a new concept. In 1887 James Moser observed that the photoelectric effect on silver plates was enhanced in the presence of erythrosine dye [21]. Throughout the 1960's, Heinz Gerischer and Rudiger Memming performed systematic mechanistic studies on ZnO [22-24] and SnO₂ [25-27] electrodes. These studies were aimed at understanding electron-transfer involving valence and conduction bands immersed in a redox electrolyte. Gerischer successfully absorbed photosensitive dye onto the surface of a stable large band gap semiconductor.

DSSCs were further advanced when bulk electron transfers were improved by introducing high surface area structures for enhancing dye absorption into the semiconducting materials. Sensitizers were eventually

developed to assist in attaching dye molecules to the mesoporous TiO₂ structures. This led to improvement in the charge injection efficiency. Grätzel and O'Regan combined these innovations with structural improvements to create the Grätzel Cell. Structural improvements occurred when the TiO₂ electrode was connected to a counter electrode with an electrolyte. The counter electrode and electrolyte provided an iodide redox system for dye regeneration [19].

2.2.2 Fundamental Operation

DSSCs are comprised of a working electrode, counter electrode, electrolyte and sealant. This project uses materials to fabricate the DSSCs that are widely accepted and trusted within the scientific community [28]. Such materials include: N719 ruthenium dye, Platisol platinum solution, Iodolyte AN-50 electrolyte, soda-lime glass with a conductive fluorine tin oxide (FTO) film, and Ti-Nanoxide D containing anatase TiO₂ nanoparticles.

The working electrode is made of dye-sensitized TiO₂ nanoparticles on a transparent conducting oxide (TCO) coated electrode. The counter electrode consists of a platinum (Pt) layer on a TCO coated electrode. The electrolyte contains iodide/triiodide (I⁻/I₃⁻) redox couple. DSSCs are majority charge carrier devices in which the electron transport occurs in the TiO₂ and the hole transport occur in the electrolyte.

The Shockley-Queisser limit is a theoretical cell efficiency limit. The difference in energy between the bandgap and photon defines the limit. If a photon contains more energy than the semiconductor bandgap, then the photoexcitation occurs. However, when photon energy is much higher than the bandgap, excess energy is lost.

Energy conversion occurs when absorbed photons excite an electron from the sensitizer dye into the conduction band of the semiconductor (generally TiO_2). A donated electron from the electrolyte restores the original state of the dye. The regeneration of the sensitizer by iodide intercepts the recapture of the conduction band electron by the oxidized dye [29]. The iodide is regenerated by the reduction of triiodide at the counter electrode through electrons, which have migrated through the external load.

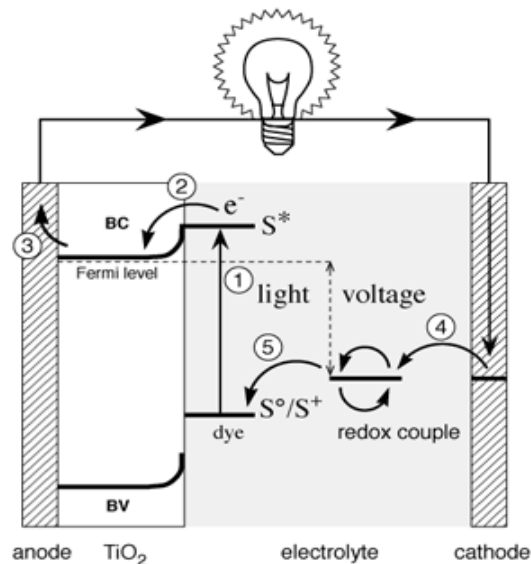


Figure 2.2: Energetic Schematic of a DSC [30]

Figure 2.2 depicts the principle operation of a DSSC and includes the energy band diagram. Holes diffuse into the n region and electrons to the p region of the semiconductor, forming an electric field at the interface. When photons are absorbed containing higher energy than the band gap, excitons are generated and transported through charge transfer. Excitons recombine unless separated by an electric field. Therefore, only excitons, which are created in the space charge layer, will contribute to the photocurrent.

The non-organic electrolytes used in the DSSC are volatile. As a result, the electrolyte becomes permeable into the encapsulation, which leads to structural and operational failure. Alternative electrolyte replacements include: organic hole conductors, semiconducting polymers [31-32], ionic conducting polymer gels [33-35], room temperature molten salts, and electrolyte gellated with amino-acid derivatives [36]. CuI [37-40] and CuSCN [41-42] have also been considered as substitutes for volatile electrolytes.

2.2.3 Structure

Figure 2.3 shows the mechanical structure of a typical DSSC. The DSSC is comprised of multiple layers stacked between two electrodes. Each electrode has a transparent conducting oxide (TCO) film, specifically Fluorine Tin Oxide (FTO) for this experiment. TiO₂ nanoparticles are sintered and bound to the FTO layer of an electrode. Dye is then absorbed

into the TiO_2 layer. Likewise, platinum nanoparticles are sintered onto the FTO layer of the opposite electrode. The two electrodes are then attached with either a two or three part liquid epoxy or a polymer sealant melt. The DSSC construction is completed with the introduction of the electrolyte into the center of the cell.

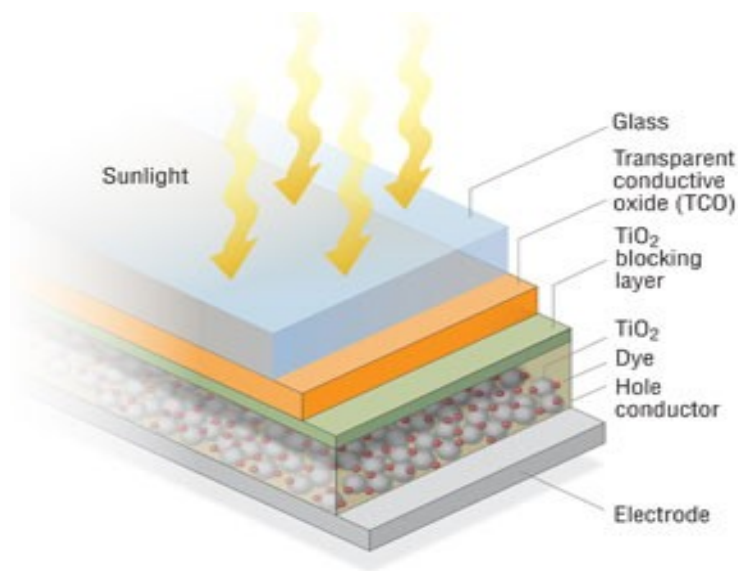


Figure 2.3: Layered components of a DSSC [43]

2.2.3.1 Glass Electrodes

Glass electrodes, also named substrates are typically made of soda-lime glass. Soda-lime glass is widely available and inexpensive, accounting for 75 % of all manufactured glass. DSSCs utilize electrodes, which have been coated with a TCO film. An assortment of thicknesses and materials can be chosen to match specified needs. The electrode is responsible for providing a low resistance path for electron transport to and from the external circuit. The glass's manufactured flatness, TCO

conductivity, and transmissivity are critical factors, which heavily effect performance of the DSSC.

2.2.3.2 Counter Electrode

The counter electrode is responsible for providing an efficient reduction reaction within the DSSC. The counter electrode usually consists of a highly conductive material coated on a glass substrate. This experiment uses two thin layers of sintered platinum on FTO coated glass. Reflective conductors and low cost copper compounds have been successfully used as counter electrodes [44-45].

DSSC efficiency is determined mostly by the rate of iodine reduction between the working and counter electrodes. For optimal efficiency, iodine must be reduced at the counter electrode much faster than the recombination rate at the TiO_2 /electrolyte interface.

2.2.3.3 Working Electrode

The DSSC working electrode contains an electrode with a conductive film and a layer of a dye-soaked semiconductor. The layer can be deposited by several different methods: sputtering, doctor blade, sol-gel [46], spraying, or electrophoretic deposition [18-19, 47-48]. The TiO_2 film is usually deposited onto a highly doped conductive film on an electrode. The conductive film and porous TiO_2 layer should have good mechanical and electrical contact to maximize the electron flow to the external circuit. The TiO_2 coating is multi-functional. It provides surface

area for dye absorption, functions as an electron acceptor for the excited dye, and also serves as an electron conductor.

Sintering the nanoparticles together is important because it allows electronic contact between the nanoparticles. TiO_2 , ZnO , SnO_2 , Nb_2O_5 , and CdSe have been studied for use as semiconducting materials in DSSCs. TiO_2 is used most frequently because of its proven stability and energetic properties that are suitable for dye attachment. TiO_2 is used in its anatase (pyramid-like crystals) low-temperature form.

2.2.3.4 Dye Sensitizer

Dye is the photoactive element attached to the TiO_2 layer to absorb incident photons. To be an effective sensitizer, the dye should cover a wide solar spectrum. Half of the solar energy falls in the 400 to 800 nm region of the visible portion (panchromatic) of the electromagnetic spectrum. The oxidation potential of the excited state of the dye should be more negative than the conduction band potential of the TiO_2 . Doing so will result in a more efficient electron injection. Likewise, the oxidation potential of the oxidized state of the dye must be more positive than the regeneration system oxidation potential. Dyes must also possess long-term stability for possible use in future commercial applications.

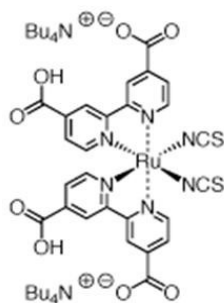


Figure 2.4: Chemical Structure of Ruthenium N719 dye [49]

The highest DSSC performances have been achieved using polypyridyl complexes of ruthenium and osmium [20]. This experiment utilizes the N719 dye complex shown in Figure 2.4. N719 is a ruthenium dye with complex $\text{cis-RuL}_2(\text{NCS})_2$. It is highly compatible with mesoporous semiconductors.

2.2.3.5 Sealant

DSSC sealants function similar to rubber gaskets in an internal combustion engine. The gaskets are used to contain and seal the energy conversion system. In DSSCs, sealants prevent the electrolyte from escaping while also providing insulation between the conductive electrodes. Polymer melts are the most commonly used sealing material; however, two or three part epoxies are also used to seal DSSCs. Sealants must be made durable to withstand the corrosive nature of inorganic electrolytes as well as to be able to remain stable during normal operating conditions.

2.2.3.6 Electrolyte

The electrolyte plays an important role in DSSCs. Performance of the DSSC is almost entirely a direct function of the semiconductor (with dye) and electrolyte quality. The electrolyte provides the oxidized dye with electrons, while the positive charge is transported to the counter electrode. The redox potential of the electrolyte must be more negative than that of the oxidized dye in order to be a functional mediator.

The electrolyte must fulfill several requirements. To avoid filtering losses, the electrolyte should not absorb significant amounts of light in the visible range. The electrolyte should also be able to effectively transport current with minor ohmic losses or diffusion limitations. Electrolyte properties must possess long-term stability qualities. Factors that affect the long-term stabilities include: chemical, thermal, optical, electrochemical, and interfacial stability.

2.2.4 Solar Cell Parameters

DSSCs and silicon solar cells function similarly, providing direct current electrical power to a load while under illumination. Likewise, standard characterization techniques are used to classify both DSSCs and silicon based cells. A few important conditions will be discussed.

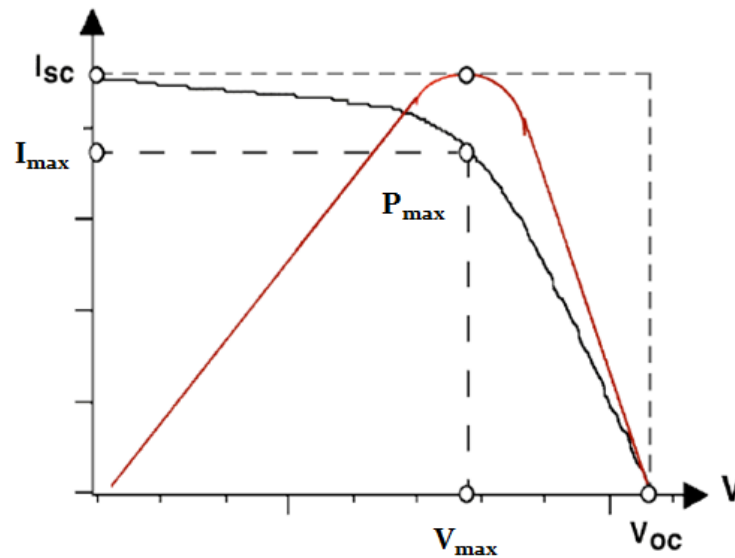


Figure 2.5: I-V Curve Characterization [50]

Short-circuit current (I_{sc}) happens when cell current is measured while a potential of zero volts is applied. I_{sc} is a direct function of the illumination intensity. Open-circuit potential (V_{oc}) is a voltage measurement when cell current is zero. Maximum power output (P_{max}) is the corresponding point where I_{max} multiplied by V_{max} is at the greatest position. Graphing current versus voltage will display an I-V curve (Figure 2.5). The maximum power output shows as the maximum power point on an I-V curve. Figure 2.5 shows this point on the I-V curve. The Fill Factor (FF) is the ratio of maximum power to I_{sc} multiplied by V_{oc} , shown in the equation below.

$$FF = \frac{I_{max} \cdot V_{max}}{I_{sc} \cdot V_{oc}}$$

Fill factor is usually a result of the series and shunt resistances within a cell. Series resistance (R_s) and shunt resistance (R_{sh}) are both

parasitic resistances that directly affect cell performance. Figure 2.6 illustrates the influence of increasing series resistance, R_s and decreasing shunt resistance, R_{sh} on the current-voltage characteristic. Optimal conditions are when R_s is as small as possible and R_{sh} is high as possible.

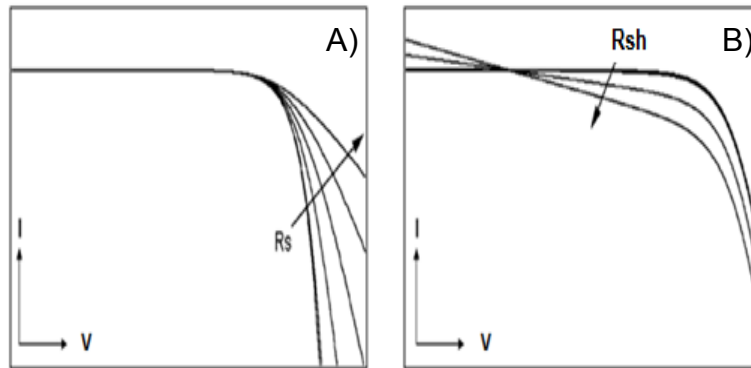


Figure 2.6: The influence of A) increasing series resistance, and B) decreasing shunt resistance on the DSSC I-V curve [50]

All the conditions mentioned within the solar cell parameters section are factors that are used to determine the cell efficiency (η). The cell conversion efficiency describes the DSSC performance and is defined as the ratio of the maximum electric power extracted to the radiation power incident on the solar cell surface. The efficiency is a function of the cell V_{OC} , the I_{SC} and the FF.

$$\eta = \frac{P_{max}}{P_{in}} = \frac{I_{sc} \cdot V_{oc} \cdot FF}{P_{in}}$$

2.3 Lean Six Sigma

2.3.1 Summary of LSS

Lean Six Sigma (LSS) is a methodology used to instill efficiency and effectiveness to a process lacking quality control. Peter F. Drucker stated, “Effectiveness is the foundation of success—efficiency is a minimum condition for survival after effectiveness has been achieved. Effectiveness is doing the right things. Efficiency is doing things right [51].” Regarding this project—quality improvement methods were utilized to make DSSC fabrication at ASU effective and efficient.

In the industrial environment, quality improvements can be expensive to implement but usually result in greater savings and increased profits for companies that apply them. Data from this study shows that Lean Six Sigma may be implemented when on a limited budget to reduce waste and defects. Procedures performed in the research laboratory for this study are almost entirely manual and at best, semi-automated. Regardless, Lean Six Sigma methods were successfully used to improve the titanium dioxide deposition process.

2.3.2 Lean Manufacturing

Lean manufacturing, also known as lean production, lean enterprise or simply Lean, is the practice of eliminating waste from the production process, which does not directly add value for the customer. Resulting benefits are prevalent in a more refined, efficient production

process. The Lean philosophy is derived largely from the success of the Toyota Production System (TPS), and popularized by the writing of Womack and Jones [52]. Early traces of waste reduction thinking can be observed in Benjamin Franklin's "Poor Richard's Almanac and the Way to Wealth [53]."

In order to achieve Lean manufacturing on a large scale production, several quality assurance tools may be employed as standard practice. Common examples of such tools are Five S (5S), Value Stream Mapping (VSM), Just-In-Time (JIT), Poka Yoke (error proofing) and Kanban (pull systems). Each tool has its own distinct purpose for improving efficiency and reducing waste.

Lean manufacturing is often considered by many to be entirely "common sense," but in actuality it requires commitment from all those involved. A quality management team usually manages it, which is led by a certified Six Sigma Master Black Belt, Champion or Executive. Lean manufacturing is responsible for reducing waste while Six Sigma enables and maintains strict process control.

2.3.3 Six Sigma

Six Sigma (6σ) consists of a compilation of quality tools used in a systematic methodology to fundamentally eliminate defects. Bill Smith originated the Six Sigma concept in 1986 at Motorola [54-56] to address Motorola's lack of manufacturing quality. Later it evolved into quality tools

and ideas through the contribution of numerous quality gurus including, but not limited to W. Edwards Deming, Joseph Juran, Genichi Taguchi, Kaoru Ishikawa, Philip Crosby, and Walter A. Shewhart [57-60]. Six Sigma gained popularity in 1995 after Jack Welch, the Chief Executive Officer of General Electric, implemented Six Sigma to improve the quality of General Electric's general manufacturing processes [54-56].

Six Sigma was first used to improve manufacturing processes by eliminating defects, but was later found to be useful in improving other processes outside production facilities. Six Sigma is mutually beneficial to both the customer and the practicing company if used correctly. Due to the continual rise of global competition, reducing defects became critical to the success of nearly every company, no matter the size.

Quality is a term defined by the customer; therefore, products are manufactured or fabricated to meet a target set to satisfy the customer. If a process functions correctly, corresponding data can be plotted to show a normal curve. Any data points that lie outside the customer's upper and lower specification limits (LSC/USL) are considered defects. Six Sigma represents six standard deviations (three in the positive or negative direction) from the customer's specified target. This is where Six Sigma's title originated, meaning six standard deviations (6σ). A successful Six Sigma process outputs 99.99966% or greater non-defective units, resulting in only 3.4 defects or less out of a million units of opportunity;

which is the ultimate achievement potential. One great benefit to Six Sigma is that process control may be numerically represented using a calculated sigma level from inputting defects per million opportunities (DPMO) into a sigma calculator. Even though 6σ is nearly impossible to obtain when manual processes are involved, a sigma level will prove useful on this project because it provides a quick gauge of how well implemented process improvements are functioning.

Six Sigma projects follow one of two methodologies inspired by W. Edwards Deming's Plan-Do-Check-Act cycle. Each of the methodologies involves five distinct phases. Define-Measure-Analyze-Design-Verify (DMADV) is meant for creating a new product or process design. Define-Measure-Analyze-Improve-Control (DMAIC) is useful for improving existing processes. DMAIC was used in this experiment to improve the Titanium Dioxide Deposition Process, which contained defects in which the causes were not known. Although Lean manufacturing and Six Sigma are separate quality practices, they share similar goals, which intermesh so effortlessly that they are commonly considered the same methodology, hence the title Lean Six Sigma.

2.4 Standard Operating Procedures

Standard operating procedures (SOPs) are used as a means of standardization—part of implementing continual improvement procedures on a process. Standardization is a highly effective method for maintaining

statistical and process control. Good laboratory practice (GLP) is a frequently practiced set of standards in the laboratory environment. GLP is a standard by which laboratory studies are designed, implemented and reported to assure the public that the results are correct and the experiment can be reproduced exactly, at any future time [61]. Although it is not required, all university and engineering laboratories should practice GLP standards [61], since SOPs are a multi-beneficial GLP component.

SOPs promote quality through improved consistency and are often used as a training tool for new personnel. Following an SOP will keep in reducing opportunities for miscommunication while also facilitating uniformity and activity compliance. Adhering to the SOP usually results in reduced work and increased quality, however, SOPs are only effective if actively updated and implemented [61-63].

The purpose of SOPs is straightforward: to ensure that essential job tasks are performed correctly, consistently, and in conformance with internally approved procedures. Ironically, SOPs are created using general guidelines, but follow no direct set of standards.

Chapter 3

EXPERIMENTAL METHODS

3.1 Fabrication Improvements

DSSC fabrication consists of four processes and three supporting sub-processes. Unsystematic process improvements may produce undesired or unrecognizable results, which equate to wasted materials, costs and time. Figure 3.1 illustrates how each process or sub-process is linked into the project. Individual processes are numbered according to the proposed order of improvement.

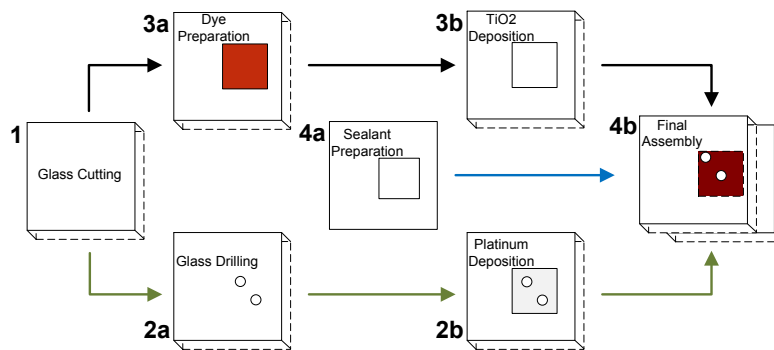


Figure 3.1: DSSC fabrication improvement flow chart

The following order of improvement applies to Figure 3.1 above:

1. Glass Cutting Process
- 2a. Glass Drilling Sub-process
- 2b. Platinum Deposition Process
- 3a. Titanium Dioxide Deposition Process
- 3b. Dye Solution Preparation Sub-process

4a. Sealant Preparation Sub-process

4b. Final Cell Assembly

All processes and sub-processes contained areas in need of improvement. Procedures took too long to perform, and the output was often unpredictable. The root causes of defects are well known for three out of the four processes and all three sub-processes. Eliminating the causes of defects within each process will drastically increase effectiveness. The root cause of defects was unknown for the titanium dioxide process. Therefore, the DMAIC methodology was used to identify and reduce the causes of defects for that process. SOPs have been created and implemented to maintain process control following the final process improvements (Appendix A). The titanium dioxide deposition process was central to the topic of this study; therefore, the titanium dioxide deposition process will be presented in an order superseding the other processes.

3.1.1 Titanium Dioxide Deposition Process

A bulk of the DSSCs activity occurs within the TiO₂ layer. Coating a layer of TiO₂ onto the working electrode is a delicate procedure. Minor deviations in procedure can lead to large changes in performance.

3.1.1.1 Titanium Dioxide Deposition Problem Statement

Fabrication flaws are considered defects, which are created during the TiO₂ coating process. Fabrication flaws cause the performance to drop

below acceptable levels. The original coating process proved to be ineffective and inefficient. The TiO₂ deposition process took a great amount of time to perform and still displayed little consistency in performance or coating uniformity. Many group discussions and various modifications have been attempted to resolve the root causes of defects or inconsistencies in the titanium dioxide deposition process.

3.1.1.2 Original Procedure

Coating procedures on this ongoing project have evolved since originating with the first graduate researcher in 2009. The procedure that was handed down from the previous researcher was by no means incorrect but had documented difficulties in coating and performance replication. The original procedural steps are described in the following summarized form:

First, the coating machine and tools were cleaned with isopropyl alcohol. After cleaning, the coating machine had to be calibrated. Because the coating machine was shared among various graduate projects, this meant recalibrating the heights for each use was required, therefore introducing extra variability between coatings.

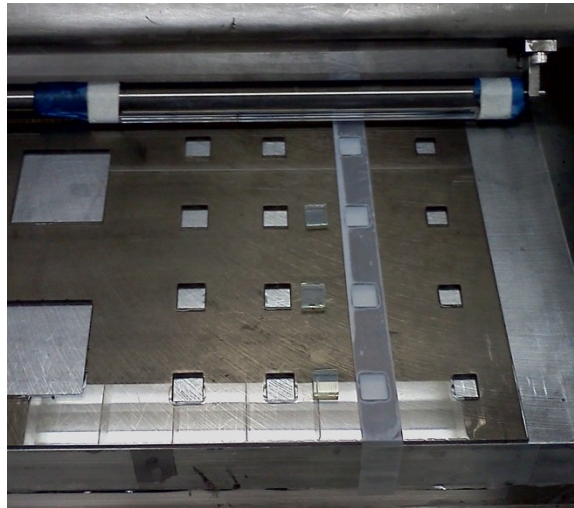


Figure 3.2: Coating TiO_2 using a glass rod

Figure 3.2 above shows the glass coating rod taped to a steel rod. The glass rod was initially used as the doctor blade, but a few months later, a steel precision doctor blade replaced the rods on the coating machine (Figure 3.3).

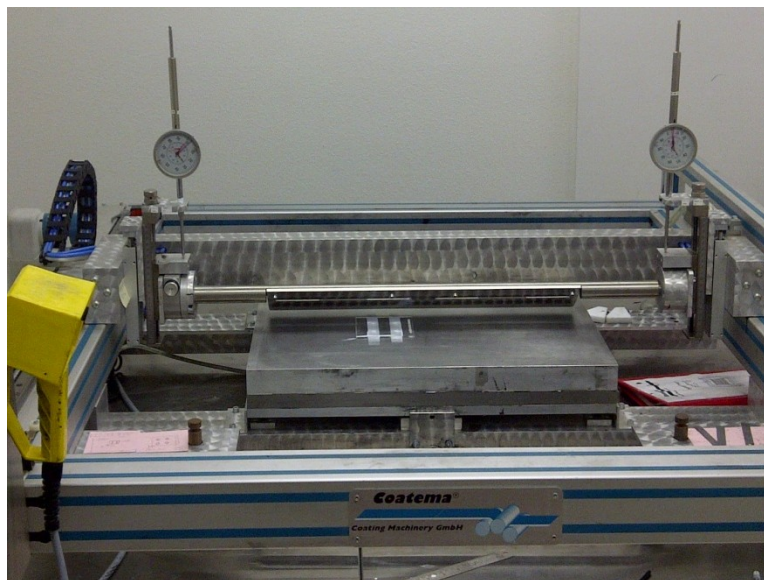


Figure 3.3: TiO_2 coating method using a steel doctor blade

The next step of the procedure was to place three layers of tape over each opening on a three-slotted 3 mm thick template. A 7 mm x 7 mm coating mask was made through the tape using the laser. The same file, template and settings that were used for making the platinum deposition mask that was also used during the TiO₂ deposition process. TiO₂ paste was placed in the ultrasonic bath to be stirred for five minutes prior to coating. Glass electrodes were placed into the template openings conductive side facing the tape. The template was then positioned on the coating machine platform.

Using a pipette, a line of TiO₂ paste was deposited above each tape mask opening. The glass rod was then advanced forward to apply the paste onto the openings of the mask. Next, a clean Petri dish lid was placed over the freshly coated layers and left to dry for ten to fifteen minutes. Electrodes were then removed from the templates and placed into the furnace inside a Petri dish for one hour and forty-five minutes at 400°C. Following the ten hour cool down time, the sintered TiO₂ electrodes were then be inserted into the dye solution.

3.1.1.3 Steps Taken to Improve Methodology

The Six Sigma DMAIC methodology was applied to the process to help identify and eliminate root causes of defects in the titanium dioxide deposition process.

In this methodology, the purpose of the project is defined by the people involved or affected. Involved parties (key stakeholders) are known as the customers. The project research team possesses the voice of the customer for the purposes of conducting the Six Sigma DMAIC process. Customers have defined the Critical to Quality (CTQ) goals as obtaining non-defective cells and minimal waste of materials.

Tools	Define (D)	Measure (M)	Analyze (A)	Improve (I)	Control (C)
Brainstorming				X	
Cause-and-Effect Diagram			X		
Control Charts				X	X
Pareto Chart		X			
Process Map	X			X	X
SOP					X
Checklist		X			

Table 3.1: DMAIC tools used to improve the Titanium Dioxide process

Table 3.1 shows various statistical or quality control tools that will be used within DMAIC to improve the TiO₂ deposition process.

TiO₂ dimensions (area and thickness) had been optimized in previous research conducted by Aung Kyaw Htun [64]; therefore, dimensions will not be modified. TiO₂ coating processes are sensitive to change. Variations in the coating process often result in a wide array of performance outputs and defects.

In the following sections (3.1.1.3.1 to 3.1.1.3.25), a series of processes were implemented to reduce or eliminate the many defects encountered in the previous original work. After each remedial process is described, an updated benchmark map and table is presented to provide progress visualization and to benchmark the process.

3.1.1.3.1 Define Phase at Benchmark #1

The Original TiO₂ deposition process map (Figure 3.4) defines how the process operated before improvements were made. This point in time is referred to as benchmark #1. The gray-shaded blocks indicate steps that frequently produced defects.

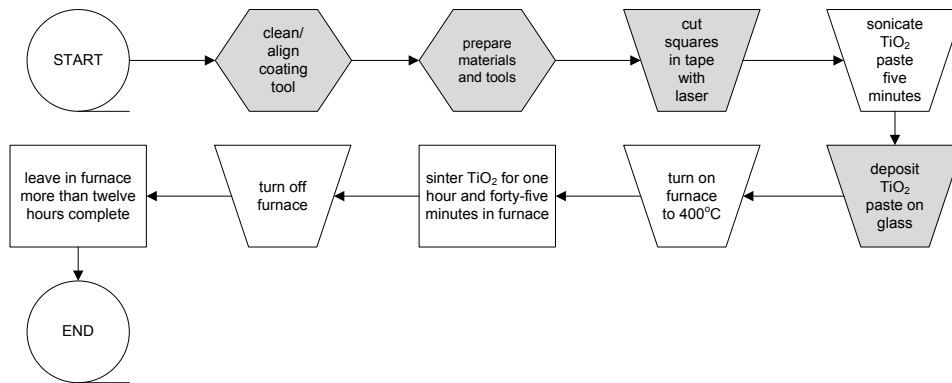


Figure 3.4: Original TiO₂ Deposition Process Map

3.1.1.3.2 Measure Phase

The DMAIC Measure stage is primarily meant to establish baseline capabilities. Therefore, this is strictly a numerical data collection stage. Data is presented as the type and occurrence of defects during the titanium dioxide deposition process. TiO₂ layer defects are imperfections that are caused during the deposition process, which lead to a non-

uniform TiO₂ layer. TiO₂ layer cracking defects are identified and classified using a microscope on the 10x magnification lens setting (Figure 3.5 below).



Figure 3.5: Microscope and monitor used to view TiO₂ defects

Defects were recorded to a checklist (Table 3.2). Each benchmark is a point in time, which stands for specific improvement stages. The first benchmark shows the occurrence of defects for fifty-six samples of TiO₂ layers during the initial deposition process prior to any improvements.

Benchmark	Cracked Corners or Edges	Minor Cracking	Severe Cracking	Skewed Thicknesses	TiO ₂ Layers vary within Batches	Number of Samples
1	42	2	0	3	8	56

Table 3.2: Checklist of defects during the initial process at Benchmark #1

Figure 3.6 shows two images of various cracking defects. Figure 3.6A is considered a mud-cracking defect. Similar to conventional paint, TiO₂ paste exhibits mud-cracking when the manufacturer's recommended

layering thickness is surpassed. Mud-cracking can also occur if contaminants are present on the surface of the glass before coating.

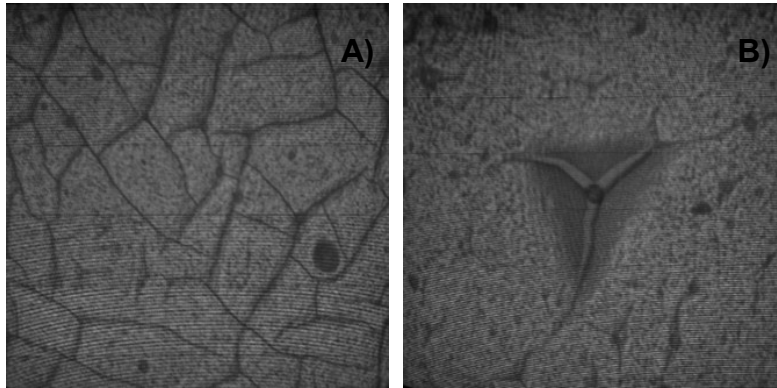


Figure 3.6: Sintered TiO_2 defect images; A) minor (mud) cracking, B) severe cracking.

Undesirable flaking (Figure 3.7) and severe cracking occurs when the TiO_2 is coated on too thin (Figure 3.6B).

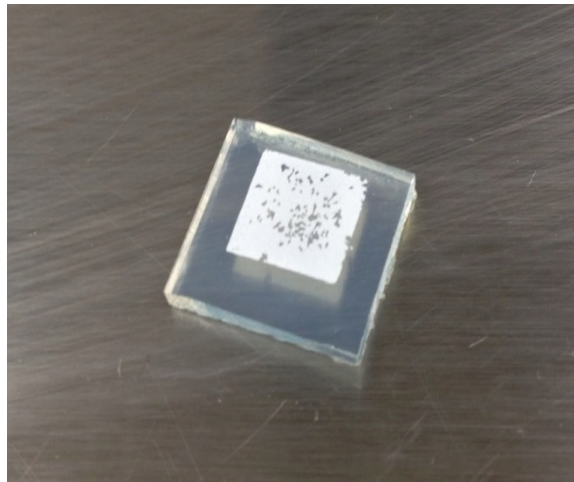


Figure 3.7: TiO_2 flaking

Sintered TiO_2 layers are visually inspected to determine the general thickness of the layers. A visual inspection is performed by viewing the

layers and categorizing the various layers of opaque contrasts. The TiO_2 layer thicknesses were organized in five different categories labeled: 1) too thick; 2) too thin; 3) skewed thickness; 4) not consistent between samples of the same batch; or 5) ideal. Any condition other than ideal represents a defect. This evaluation was performed with limited access to precision equipment; otherwise, more accurate methods for measuring material thicknesses would be utilized.

Figure 3.8 is a Pareto Chart of the defects produced during the initial process. Pareto Charts allow visual conception of the defects within the process. Data that has a normal distribution can be placed into Pareto Charts, which usually follows the 80/20 rule. For this experiment, the 80/20 rule implies that roughly 80 % of the defects are created by 20 % of the causes.

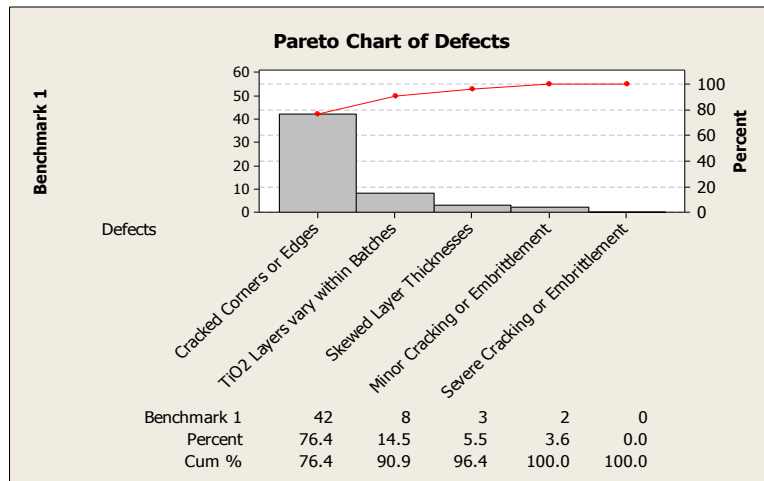


Figure 3.8: Pareto Chart of initial TiO_2 deposition process

3.1.1.3.3 Analyze Phase

Defects may now be analyzed. Data from the Checklist (Table 3.2) and Pareto chart (Figure 3.8) shows that the leading cause of defect is “Cracked Corners or Edges.” These defects accounted for 76.4 % of all the initial process defects. Once the leading defect is identified, the cause must be identified in order to make improvements. Using Cause-and-Effect diagrams will not directly locate the root cause of defects but will help to depict possibilities. There are two possibilities identified on the branch of “Cracked Corners or Edges” on the Cause-and-Effect Diagram (Figure 3.9) that could lead to a high amount of defects. Resolving the coating pressure indifferences should correct both the “Skewed Thicknesses” defects and “Excessive pressure on the tape mask” cause of the “Cracked Corners or Edges” defects.

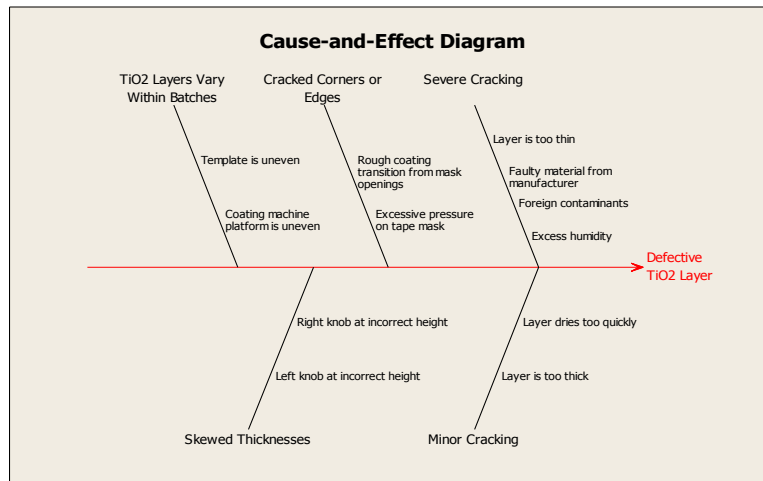


Figure 3.9: The Cause-and-Effect Diagram for TiO₂ Deposition Defects

3.1.1.3.4 Improve Phase

The main objective of this stage is to prove that the improvement instituted to address the root cause worked properly. The first improvement involved using 0.025” shims to calibrate the left and right doctor blade heights off of the coating template. Another improvement was made by creating a standard laser cutting file for the coating mask. This mask improvement mostly affects the active layer alignment during the final assembly process, but also shortens the time it takes to cut a mask in the titanium dioxide process.

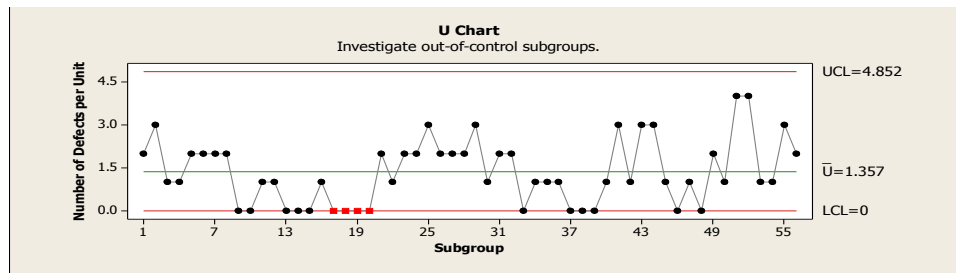


Figure 3.10: U Chart prior to the first improvement

Figure 3.10 is a U Chart that shows the number of defects per sample prior to the calibration change. The mean number of defects per sample was 1.357. The figure below shows that after implementing improvements on twenty-four samples, the mean decreased to 0.958 defects per sample—a clear improvement.

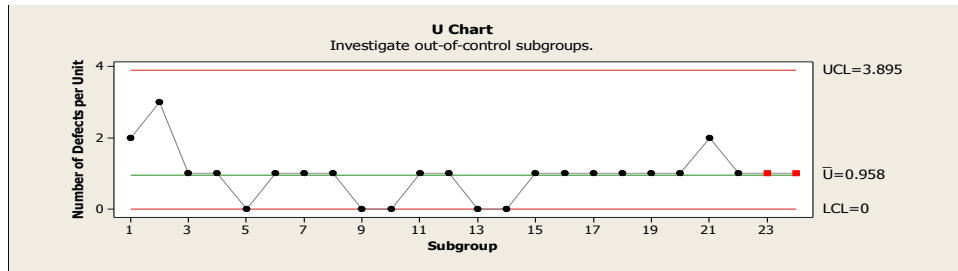


Figure 3.11: U Chart after the first set of improvements

Figure 3.12 below is an image of coated TiO_2 after implementing the first set of improvements. The image shows that the two outside TiO_2 layers are slightly thinner than the middle two layers. This is evident by the slight contrast in the opaque color. The TiO_2 layer to the farthest right shows that the edges are thinner than the middle of the layer.

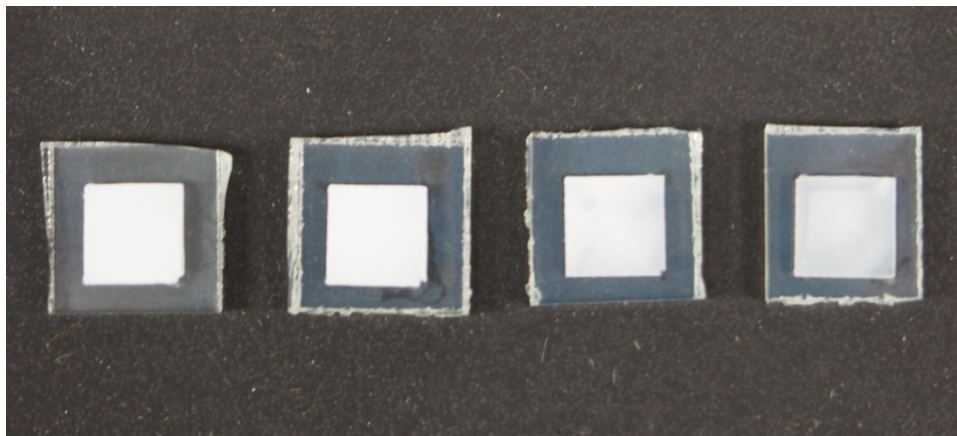


Figure 3.12: TiO_2 layers following the first set of improvements

3.1.1.3.5 Control Phase

Once an improvement has been made, it must be maintained. Standardizing the process is important. Improvements are benchmarked on process maps, which outline the entire process. The Process Map (Figure 3.13) below shows that while improvements were made to the

alignment of the coating tool and cutting of the tape mask, there are still defects caused at other steps of the process.

DMAIC is a revolving method that allows improvements to be made as needed following the Control stage. Further improvements will need to be made to the deposition process until it becomes capable of consistently producing defect free samples. A SOP must be used to maintain process control after final improvements are made to this experiment.

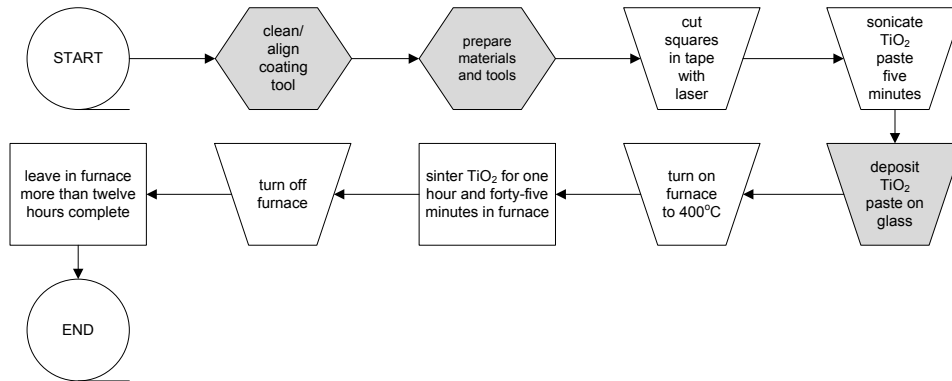


Figure 3.13: Process Map following the first set of improvements at Benchmark #2

3.1.1.3.6 Define Phase at Benchmark #2

The previous U Chart (Figure 3.11) shows that defects still exist within the titanium dioxide deposition process. Another round of improvements is needed to remedy further causes of defects.

3.1.1.3.7 Measure Phase

Table 3.3 is the checklist of defects that occurred to samples following the first set of improvements.

Benchmark	Cracked Corners or Edges	Minor Cracking	Severe Cracking	Skewed Thicknesses	TiO ₂ Layers vary within Batches	Number of Samples
2	13	5	3	0	8	24

Table 3.3: Checklist of defects (Benchmark #2)

These defects are listed on the Pareto Chart (Figure 3.14) by frequency to illustrate the distribution of defects recorded at the second benchmark.

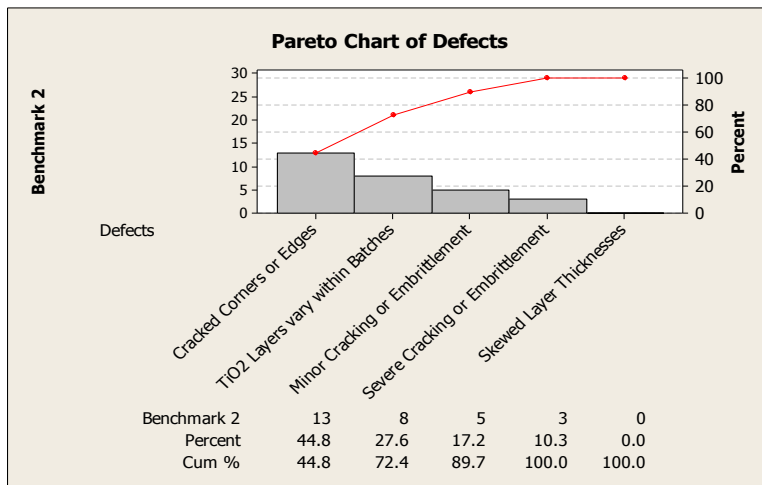


Figure 3.14: Pareto Chart at Benchmark #2

3.1.1.3.8 Analyze Phase

According to the Pareto Chart (Figure 3.14) and Checklist (Table 3.3) above, “Cracked Corners or Edges” are still the leading defect. The “Cracked Corners or Edges” can properly be addressed now that the other alternative cause was eliminated during the previous improvement. Rough coating transitions happen when the horizontally progressing blade meets the horizontal edge of the tape mask. The gradient transition is rarely smooth.

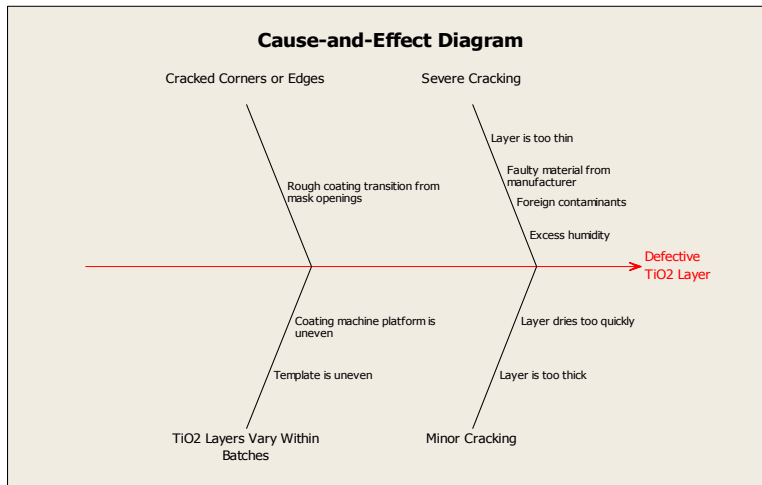


Figure 3.15: The Cause-and-Effect Diagram at Benchmark #2

3.1.1.3.9 Improve Phase

Through means of brainstorming, new coating templates were fabricated using diamond shaped openings instead of square shapes. This improvement provided a smoother transition between the edges of the tape and the doctor blade, therefore minimizing thickness gradients on the corners and edges of the TiO_2 layers. The U Chart in Figure 3.16 shows that the mean number of defects per unit increased from 0.958 to 1.5; however, the consistency between samples greatly improved. Lean Manufacturing 5S methods were installed at the same time as the improvements to the coating template were made.

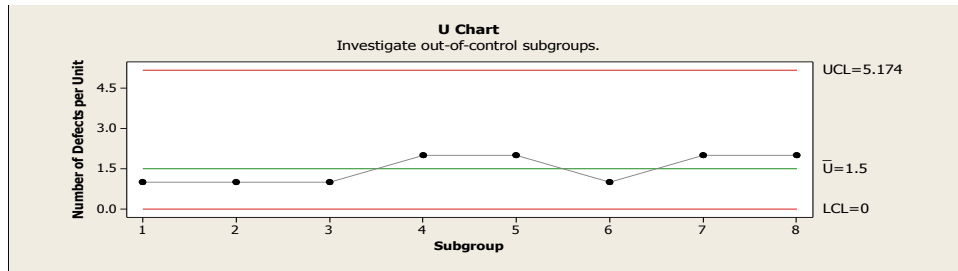


Figure 3.16: U Chart after the second set of improvements

Figure 3.17 below shows that the using diamond shaped openings in the template eliminated defects on the edges and corners of the layers.

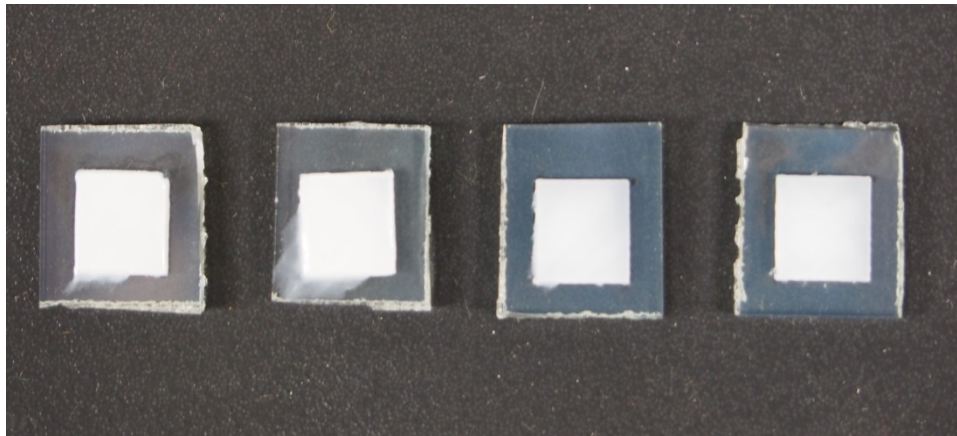


Figure 3.17: TiO₂ layers following the second set of improvements

3.1.1.3.10 Control Phase

Consistency in defect variation was improved, but the total number of defects per sample still remained too great. Utilizing the 5S method helped improve procedure consistency and removed issues pertaining to the “prepare materials and tools” step of the titanium dioxide deposition process. However, an additional round of improvements still needs to be implemented.

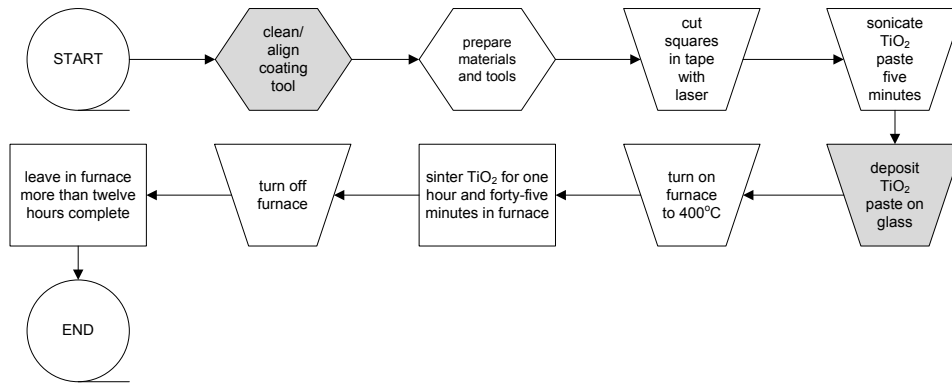


Figure 3.18: Process Map following the second set of improvements at Benchmark #3

3.1.1.3.11 Define Phase at Benchmark #3

There are still three variations of defects that continue to arise from two steps of the titanium dioxide deposition process: TiO₂ layers that vary between batches, severe cracking or embrittlement, and minor cracking or embrittlement.

3.1.1.3.12 Measure Phase

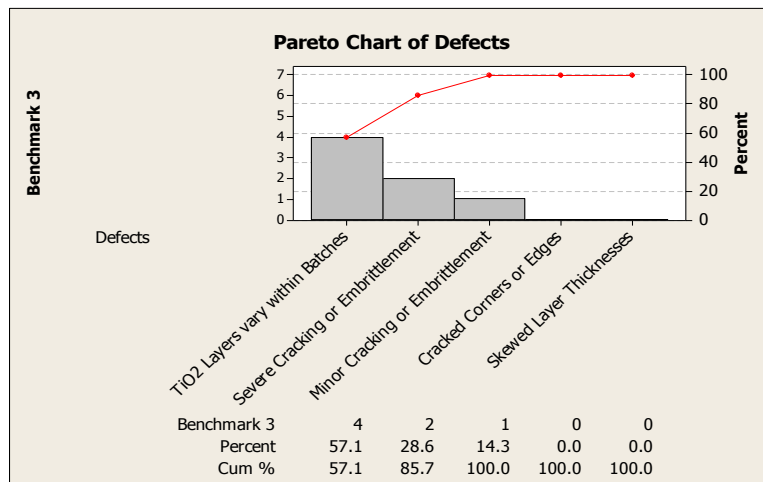


Figure 3.19: Pareto Chart at Benchmark #3

3.1.1.3.13 Analyze Phase

Benchmark	Cracked Corners or Edges	Minor Cracking	Severe Cracking	Skewed Thicknesses	TiO ₂ Layers vary within Batches	Number of Samples
3	0	1	2	0	4	8

Table 3.4: Checklist of defects at Benchmark #3

Table 3.4 presents the number of occurrences of defects following the second round of improvements at benchmark #3. Time constraints that month only allowed for fabrication of eight samples. Having small quantities of samples does not allow for accurate interpretation of trends due to greater chance of experimental error to occur. That is why an acceptable amount of experimental error is normally considered to be less than 5 %. Without twenty samples it is hard to approach an accurate conclusion from the results of the data. However, deadlines approached and further improvements were still needed.

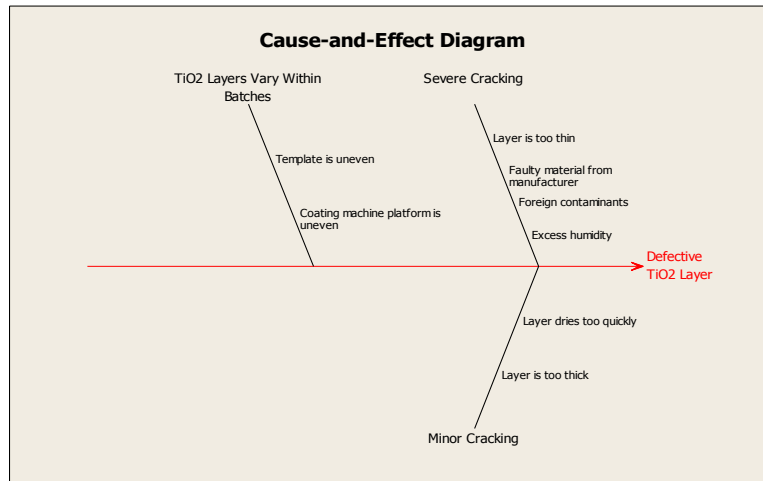


Figure 3.20: The Cause-and-Effect Diagram for Benchmark #3

The Pareto Chart and Checklist show that the highest amount of defects after eliminating the “Cracked Corners or Edges” defect remains to

be that “TiO₂ Layers Vary Within Batches.” The Cause-and-Effect Diagram (Figure 3.20) shows that there is a flatness discrepancy in either the template or the coating machine platform.

3.1.1.3.14 Improve Phase

A modification to the placement of the template on the coating machine platform needed to be made. The coating machine platform was determined to be uneven. The template was placed at a coordinate on the platform that appeared to be uniform. The position of the template was then marked on the platform. Tests for uniformity were then performed using old TiO₂ material. This was repeated several times until an acceptable position was acquired on the platform.

Results from the U Chart (Figure 3.21) below display a considerable decrease in variability and overall number of defects. The mean number of defects per sample decreased to 0.636 in a population of forty-four samples. This was a significant improvement over the last set of data, which had a mean of 1.5 defects per sample.

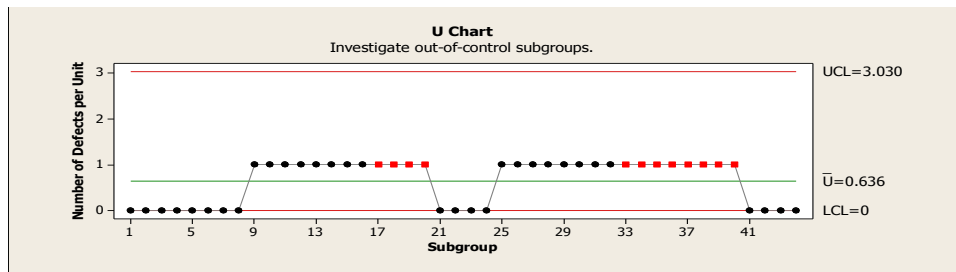


Figure 3.21: U Chart after the third set of improvements

Figure 3.22 below illustrates that layer thicknesses are now consistent within the same batch. This is an indication that implementing a standard position on the coating platform corrected TiO₂ layer inconsistencies within the same batch.

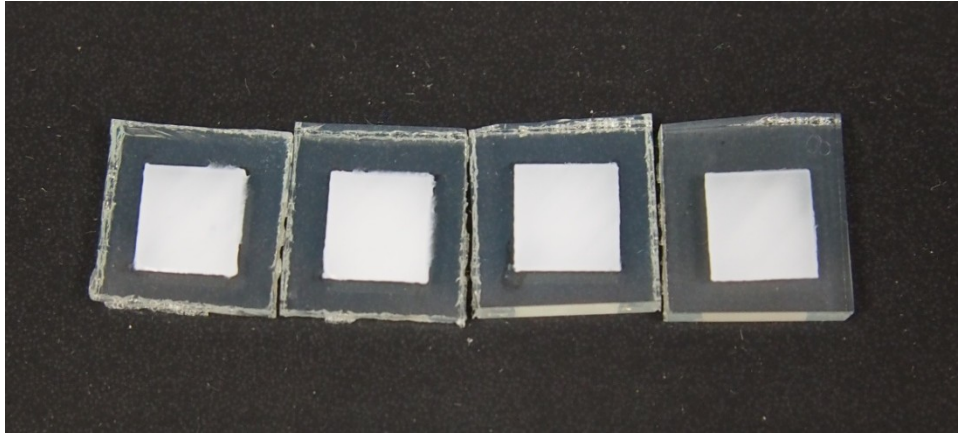


Figure 3.22: TiO₂ layers following the third set of improvements

3.1.1.3.15 Control Phase

The Process Map below illustrates that the process is nearly free of defect originating steps. One last set of improvements would be implemented to resolve the inconsistency in TiO₂ layer thicknesses between batches.

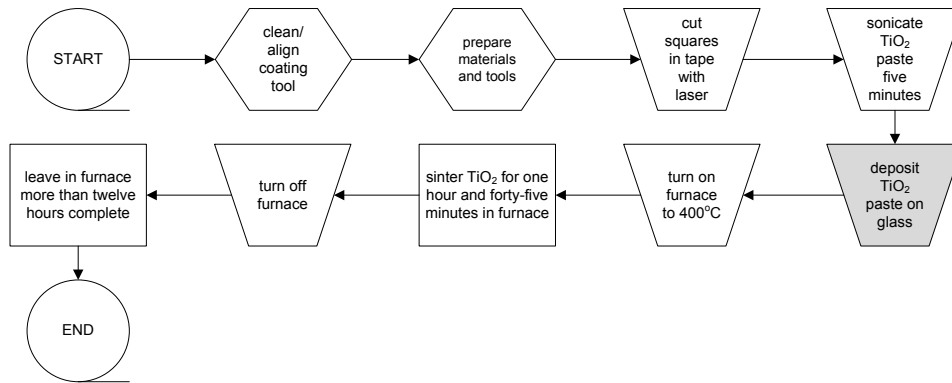


Figure 3.23: The Process Map following the third set of improvements at Benchmark #4

3.2.5.3.16 Define Phase at Benchmark #4

The process has been greatly improved but still produces defects in nearly half of the fabricated TiO₂ layers. The Process Map in Figure 3.23 shows only one remaining step that requires modification before proper control is established.

3.1.1.3.17 Measure Phase

Benchmark	Cracked Corners or Edges	Minor Cracking	Severe Cracking	Skewed Thicknesses	TiO ₂ Layers vary within Batches	Number of Samples
4	0	8	4	0	0	48

Table 3.5: Checklist of defects at Benchmark #4

The Checklist of defects occurring after the third set of improvement is displayed in Table 3.5. Below in Figure 3.24 is the Pareto Chart of the defects involving two types of cracking or embrittlement.

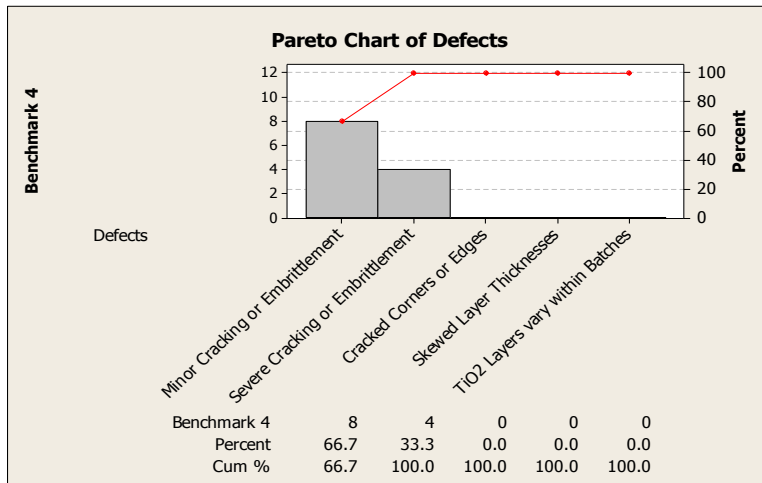


Figure 3.24: Pareto Chart at Benchmark #4

3.1.1.3.18 Analyze Phase

The following Cause-and-Effect Diagram displays those two remaining defects, which lead to a defective TiO₂ layer. Cracking can appear for several different reasons; however, the two cracking defects are usually caused from inconsistent layer thicknesses. The tape mask should determine the thickness of the layer. Regardless, the layer thickness is ultimately defined by the height of the doctor blade. The doctor blade is extremely rigid, whereas the tape mask is pliable. Resolving this issue should cure the differences of TiO₂ layer thicknesses.

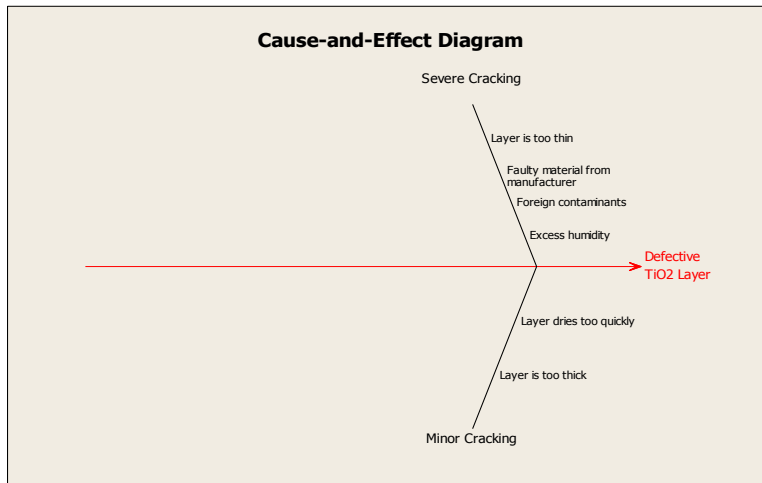


Figure 3.25: The Cause-and-Effect Diagram for Benchmark #4

3.1.1.3.19 Improve Phase

Manually coating is a common method in DSSC research projects. A 5 cm x 5 cm sheet of glass is used in place of the large steel doctor blade. The glass is pulled at a 45° lagging angle, similar to the previous method (Figure 3.26 below). Pressure is kept minimal so that the thickness of the tape dictates the thickness of the layer. The process is simple yet effective.

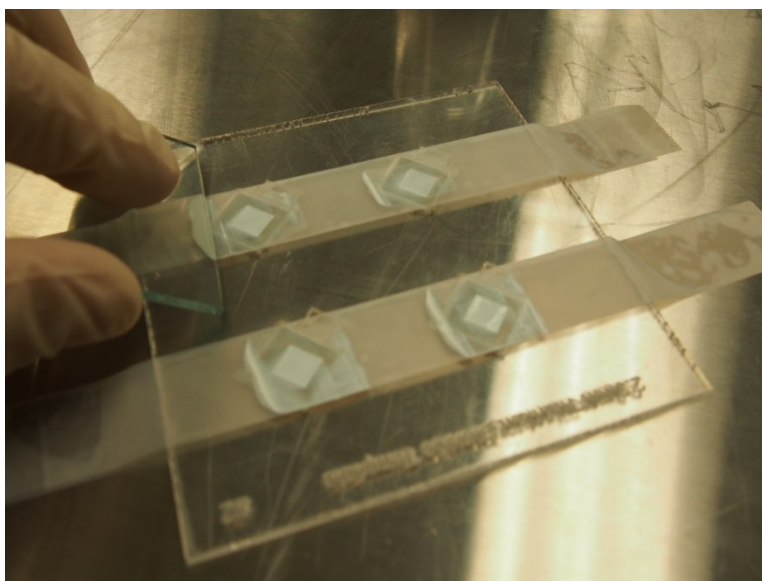


Figure 3.26: TiO₂ hand coating method

Figure 3.27 is an image of the uniformly hand coated TiO₂ layer using the microscope at 10x magnification.

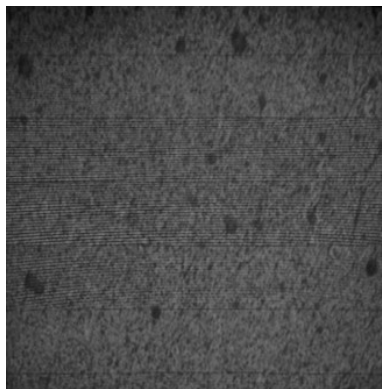


Figure 3.27: A hand coated TiO₂ layer after sintering

Table 3.6 shows that twenty individual electrodes were coated with no defects. This was a clear improvement over the previous method. Layers could be deposited more accurately in a fraction of the time.

Benchmark	Cracked Corners or Edges	Minor Cracking	Severe Cracking	Skewed Thicknesses	TiO ₂ Layers vary within Batches	Number of Samples
5	0	0	0	0	0	20

Table 3.6: Checklist of defects at Benchmark #5

Figure 3.28 below shows consistent layers fabricated by using the hand coating method. The layers are the correct thickness with no signs of defects.

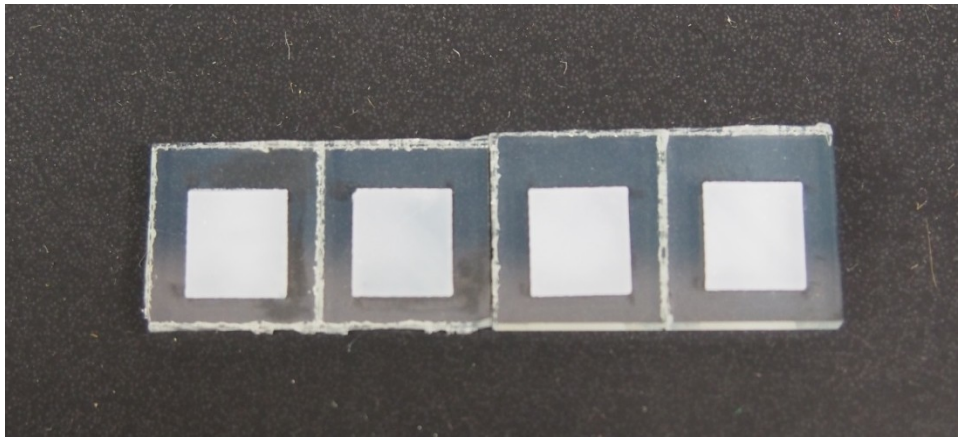


Figure 3.28: TiO₂ layers following the fourth set of improvements

3.1.1.3.20 Control Phase

Figure 3.29 shows the Process Map of the titanium dioxide deposition process after all improvements were implemented. An SOP is now utilized to maintain the improved procedures and ensure that process control is upheld. The complete fabrication process is included in the SOP listed in Appendix A.

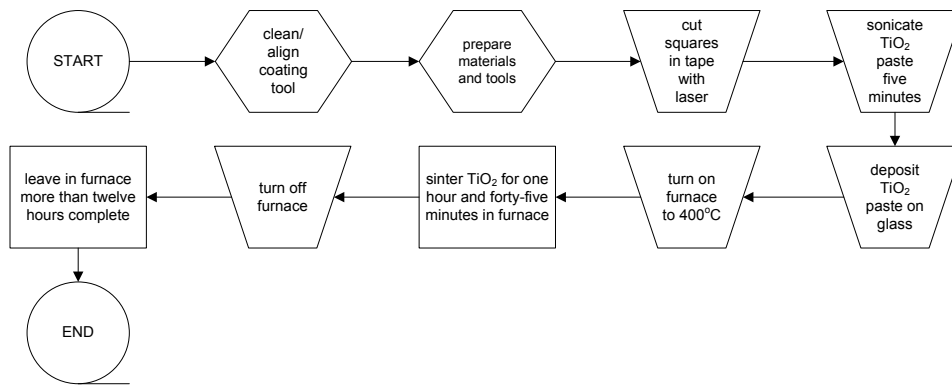


Figure 3.29: Process Map following the fourth set of improvements at Benchmark #5

3.1.2 Glass Cutting Process

Glass cutting is the first step in the fabrication process. The procedure was developed by previous research students, but was a process that needed improvement. Soda-lime glass is multifunctional. It doubles as protection for the active components while also serving as a platform to house both the titanium dioxide and the platinum layer. Fluorine doped Tin Oxide (FTO) conductively coated soda-lime glass is offered by manufacturers in thicknesses of 2.2 mm, 2.3 mm or 3.0 mm. The thickness of the glass will dictate the transmissivity quality. Increased transmissivity allows for better photon penetration, but at the same time it increases heat within the cell active area.

The FTO conductive layer functions as the electron transport mechanism for the anode and cathode of the cell. FTO layers are available for purchase in different thicknesses as well. Thicker FTO coatings have higher ohmic resistance, while still providing adequate

durability to heat and physical damage. Thinner FTO layers are susceptible to physical damage. On the other hand, the thinner layers demonstrate heightened performance. FTO coated glass is available in lengths and widths of either 5 cm x 5 cm or 10 cm x 10 cm sheets. Several different cutting methods exist for the glass. A cutting laser was utilized to minimize the damage to the FTO layer and to ensure straight, controlled cuts.

3.1.2.1 Glass Cutting Problem Statement

The quality of the glass substrates (pieces) largely determines the results of the other processes. The original glass cutting process produced inaccurately cut substrates and was wasteful. In addition, correctly sized glass would often have damaged conductive layers due to excessive movement on the laser tray during the cutting procedure.

3.1.2.2 Original Procedure

The original cutting procedure involved an acrylic positioning template, 5 cm x 5 cm sheets of 3.0 mm thick FTO layered soda-lime glass, a laser cutting machine, and a desktop computer loaded with CorelDRAW® 12 software.

A sheet of glass was placed with FTO layer down in the opening of the template and placed in the upper left corner of the laser tray. The vertical cutting file was opened in CorelDRAW® 12. The file was then printed with the power at 58 %, speed at 5.4 %, and pulses per inch (PPI)

at 605 PPI. The “Start” button was pressed three times for the first cut. Next, half of the glass was removed from the template and the other half was turned horizontally. The “Start” button was pressed two times. The glass was cut into halves, until sizes roughly 12-13 mm were produced. One 5 cm x 5 cm sheet of glass required twenty-three passes by the laser to produce sixteen glass substrates; each laser pass took one minute and forty-five seconds.

Individual glass substrate dimensions were measured and recorded. The ideal size substrate is 12.5 mm length x 12.5 mm width to fit the 13.0 mm length x 13.0 mm width openings in the templates used in both the TiO₂ and platinum deposition processes. Measurements were collected using a metric micrometer. Glass substrates are considered defective if the pieces possess imperfections that will negatively affect the performance of the cell. Defects include: 1. jagged edges; 2. scratched conductive layers; or 3. lengths or widths that are not 12-13 mm.

3.1.2.3 Steps Taken to Improve Methodology

Larger 10 cm x 10 cm sheets of 2.3 mm thick glass were purchased domestically to replace the previously used 5 cm x 5 cm sheets of 3.0 mm thick imported glass. These changes reduced shipping and material costs while also increasing aesthetics and performance of the DSSCs. To accommodate the larger 10 cm x 10 cm sheets of glass, new acrylic laser positioning templates and CorelDRAW[®] 12 files were created. The

CorelDRAW[®] 12 file was altered to program the laser to make all the horizontal cuts in a single command, and the entire vertical cuts on the next command. Settings had to be changed to the following: power at 55 %; speed at 5.0 %; and pulses per inch at 600 PPI.

The laser cutter was cleaned to improve functionality. It was relocated and connected to a fume hood to allow for proper ventilation. The glass in the new template was positioned on the laser tray in the same manner as the original procedure. After incorporating the thinner glass and updating the CorelDRAW[®] 12 files, the laser could efficiently cut the horizontal and vertical passes in only seven minutes and forty seconds each, resulting in fifteen minutes and twenty seconds to cut sixty-four substrates. These were significant improvements over the one minute and forty-five seconds original process. However, a negative effect occurred from using the larger 10 cm x 10 cm sheets of glass. Larger sheets of glass absorb greater quantities of heat while cutting, which often created large diagonal cracks across the entire area of a glass sheet. A variety of laser settings were attempted to resolve the problem, such as increasing the cutting speed and reducing the power. Regardless of the changes, the negative cracking effects continued.

After depleting the supply of 10 cm x 10 cm sheets of FTO layered glass, they were replaced with smaller 5 cm x 5 cm sheets. A new acrylic template was created to secure the glass in a fixed position on the laser

tray. The CoreIDRAW[®] 12 settings from the 10 cm x 10 cm glass sheets were applied to a new file for the 5 cm x 5 cm sheets. The laser was now able to cut each of the horizontal and vertical sets of lines in two minutes and forty-five seconds each, totaling five minutes and thirty seconds for the entire 5 cm x 5 cm sheet.

3.1.3 Glass Drilling Sub-process

The counter electrode consists of a glass substrate with a thin layer of platinum nano-particles. Glass drilling is a sub-process of the platinum deposition process. Each counter electrode will have one or two drilled cavities for injecting electrolyte. The cavities serve as entry paths for electrolyte after assembly. One or two cavities must be drilled through the counter electrode prior to the platinum deposition process.

3.1.3.1 Glass Drilling Problem Statement

Original drilling procedures required artisan skills to perfect. The process took roughly five minutes per electrode. The glass survival rate was low due to the fact that drilled cavities were difficult to correctly align and often cracked. Electrode conductive layers were frequently damaged due to abrasion against glass particles that settled on the bottom of the Petri dish.

3.1.3.2 Original Procedure

A Petri dish filled half full of water was placed on the platform directly below the path of the high speed drill bit. The purpose of the water

was to avoid stress cracks to the electrodes by absorbing and dissipating the heat while drilling. The drill was then loaded with a #60 solid carbide drill bit. An electrode would then be placed in the water and securely held down with the left hand thumb and index finger. The right hand would then be used to turn on the drill press and lower the armature. A cavity would be drilled half way through the glass electrode at an estimated point where the active area would eventually be coated. The electrode was then flipped over and the cavity completed through the conductive layered side. Cavities were not drilled all the way through to prevent blown-out back areas in the glass. The electrode would then be placed in a dry Petri dish and the next electrode would be drilled.

3.1.3.3 Steps Taken to Improve Methodology

Priority was given to resolving the causes of the conductive surface damaging process and lengthy drilling process. Other considerations are given to minimizing the size of the cavity to increase the active surface area of the platinum layer.

The first improvement method was introduced by experimenting with various sizes of solid carbide drill bits. The prices of the solid carbide bits are negligible at seventy-five cents to one dollar per bit. #80 solid carbide bits were tried first. These small sized bits frequently cracked the glass or ended in broken bits left in the middle of the glass. Improvement was still needed.

The next sampled drill bit size was #77. The #77 drill bits worked well. The diameter of two #77 bits is smaller than #60 bit. A decision was made to incorporate two cavities to allow for improved injection of the electrolyte. A square stencil the size of the 7 mm x 7 mm active area and a felt marker was utilized to mark the drilling position on the non-conductive side of the electrodes.

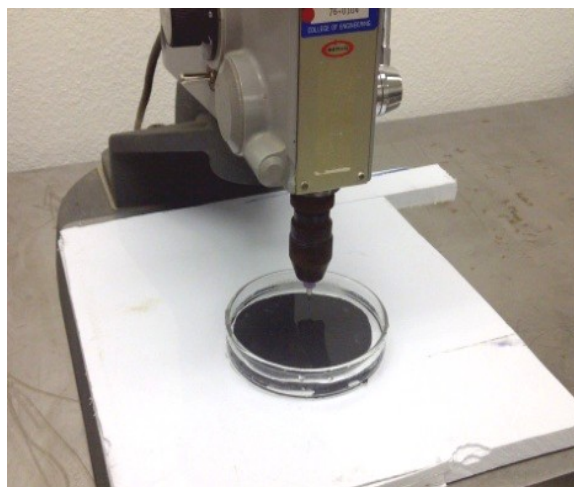


Figure 3.30: Drilling setup

The newly improved procedure begins by marking the electrodes. An electrode is then secured, conductive layer facing upwards in a Petri dish half filled with water, as in the original procedure. The two cavities are then drilled all the way through the electrodes, while ensuring that drilling pressure to the electrode is reduced near the end of the cavity to minimize blowing out the back of the glass. Some small glass blowouts are actually desirable, creating an extra area within the cavity to hold electrolyte. However, large blowouts make it difficult to create an airtight seal.

3.1.4 Platinum Deposition Process

This project uses the doctor blade deposition technique because it was found to be less damaging to the FTO layer than sputtering [1]. The counter electrode's main purpose is to efficiently re-introduce electrons from the external circuit to the electron-depleted dye. Therefore, platinum nano-particle uniformity is very important.

3.1.4.1 Platinum Deposition Problem Statement

In the original process, the doctor blade technique worked well for deposition, but the supporting process negatively impacted the uniformity of the coated layers. Unevenly dispersed layers of platinum occurred because of the large diameter of the drilled cavity in the counter electrode. A funneling effect made the platinum settle heavily on the outside edges while thinning closer to the centrally drilled cavity. The platinum layers were not consistently located on the electrodes due to the effects of the laser cutting procedure on the tape masks.

3.1.4.2 Original Procedure

The procedure was not complex. Two layers of Magic[®] tape were placed over an acrylic template with three slots. Next, a 6.5 mm x 6.5 mm opening was cut out of the two layers of tape using the laser. The position of the active area in CorelDRAW[®] 12 had to be constantly adjusted to find a somewhat correct cutting position on the two layers of tape. The laser tray and laser height were not in a fixed position, therefore, causing

inconsistent cuts on the tape masks. A coating mask was eventually created. A glass substrate was then placed in each of the three template openings, FTO layer facing the tape mask. Two drops of platinum solution were placed directly above each electrode and then quickly pulled over the electrodes using the doctor blade technique. One last thin layer of platinum solution was added over the first. The ethanol from the solution dried within five minutes of coating, leaving only the platinum nanoparticles. Electrodes were then transferred from the template to a Petri dish to be sintered at 400°C for one hour and forty-five minutes, which finalized the process. The platinum coated counter electrodes were used within twenty-four hours of sintering or reactivated by reheating at 120°C for fifteen minutes.

3.1.4.3 Steps Taken to Improve Methodology

To resolve the misalignment issue of the coating masks, the laser tray is placed in a fixed position, resting in the upper-left most corner of the laser. An improved 2.3 mm thick acrylic template is made to fit up to eight electrodes, which could be up to 14 mm in length or width, instead of the previous 13 mm size. Improvements made in glass cutting, glass drilling, and mask cutting procedures allow the newly modified platinum deposition process to run more efficiently.

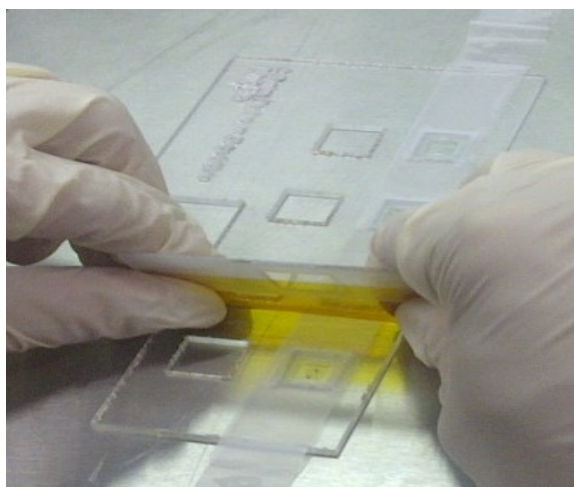


Figure 3.31: Coating Platisol on electrodes

The modified process begins by placing two layers of tape over the new template. A mask is then cut in the tape using the laser. Electrodes are placed conductive side facing up, snug and centered against the bottom portion of the template openings. Two drops of Platisol platinum solution are added above each electrode on the tape mask. A plastic squeegee used as the doctor blade is then dragged at a 45° lagging angle over all of the electrodes, top to bottom as shown in Figure 3.31. One more layer of platinum solution is added and allowed to dry for five minutes. The electrodes are then placed in a Petri dish and sintered at 400°C for one hour and forty-five minutes. The counter electrodes are then ready for use in the final assembly process within twenty-four hours.

3.1.5 Dye Solution Preparation Sub-process

The dye solution preparation is a sub-process of the titanium dioxide deposition process. Sintered TiO₂ layers must soak in a dye

solution in order to possess photon absorbing abilities. Dye solution is a mixture of N719 ruthenium dye granules in pure ethanol solvent. Making the dye solution is simple; maintaining its original composition is difficult.

3.1.5.1 Dye Solution Preparation Problem Statement

The original sub-process of preparing dye-solution was not effective. Time and expensive dye were wasted due to the evaporation of ethanol. Use of a prepared dye-solution was originally limited to one to two weeks at most.

3.1.5.2 Original Procedure

The process originally began by combining 12.3 mg of N719 dye with 40 ml of at least 99.99 % pure ethanol in an 80 ml scientific beaker. A sheet of wax paper was then placed over the top of the beaker to seal it. The beaker was stirred in an ultrasonic bath for five minutes. The contents were then poured into a Petri dish and covered with two sheets of wax paper. The Petri dish lid was placed over the sheets of wax paper. TiO₂ coated electrodes would later be added to the solution.

3.1.5.3 Steps Taken to Improve Methodology

The root cause of the problems explained in section 3.1.5.1 was that ethanol evaporates at an accelerated rate if not properly sealed. Wax paper does not provide an adequate airtight seal over the Petri dish. Due to the hastened evaporation rate of ethanol, the volume of the dye solution

could drop below the top height of the electrodes and no longer completely cover them.

Sterilized short and sealable wide-mouth jars replaced the Petri dish and beaker in the process to resolve the problem. A quantity of 6.12 mg of N719 dye is measured and placed directly into a sterilized jar; 20 ml of ethanol is then added to the same jar. The jars twist top lid is then secured on top and placed into the ultrasonic bath for five minutes. Following the stirring, the dye solution is then ready for the TiO₂ coated electrodes. The improved process works well.

3.1.6 Sealant Preparation Sub-process

Sealant preparation is a sub-process of the final assembly process, which does not require the use of DMAIC. Airtight sealing is crucial to the overall functionality of the cell. Sealants will be used to hold the working and counter electrodes together while also serving as an electrolyte containment gasket. Sealant failures result in undesirable decreases in durability and reliability, and in extreme cases—electrode separation.

3.1.6.1 Sealant Preparation Problem Statement

Electrolyte vapors manage to escape from most of the DSSCs. The original procedure did not produce uniformly sized sealants.

3.1.6.2 Original Procedure

The procedure began by cutting a 16 mm strip of 25 µm thick Surlyn[®] sealant from a larger sheet using scissors. The strip of sealant

was further reduced into 15-16 mm wide squares. Central squares, 6.25 mm x 6.25 mm in size, were cut using a precision blade and side of a metal ruler.

3.1.6.3 Steps Taken to Improve Methodology

Two options are available for bonding the working and counter electrodes together—two or three part epoxies or polymer-based sealant melts. This experiment utilized polymer sealant melts. Improvement emphasis was placed upon creating a standard sized sealant in less time. Square metal stamps were first explored as a possible solution. The stamps did not cut through the polymer sealant material—only stretched it. Having a sharp cutting stamp machined to the correct dimensions would have been a valid solution, but would exceed the project budget.

Bynel[®] 60 μm thick sealant replaced the Surlyn[®] 25 μm thick sealant. This increased the ability to handle and cut the sealant. Now, 16 mm x 16 mm squares of 60 μm thick sealant are accurately cut using a paper trimmer. The inner square is easily cut using a size #17 X-Acto[™] chisel blade and a square stencil (Figure 3.32).

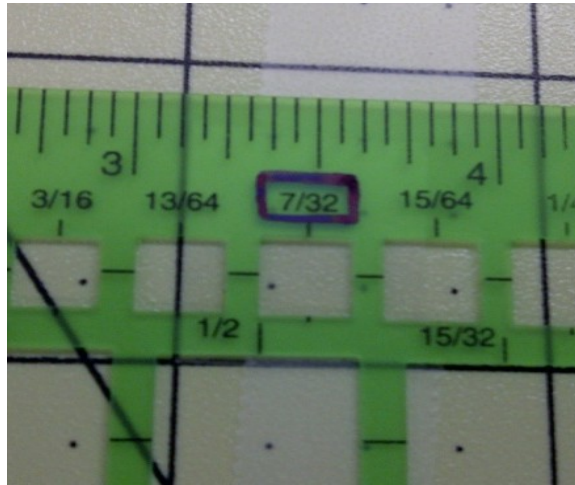


Figure 3.32: Sealant cutting procedure

3.1.7 Final Cell Assembly Process

Final Assembly is a lengthy manual procedure. Mistakes made during assembly usually result in non-working cells. Non-working cells amount to loss in time, materials and costs. It remains imperative that researchers take as much time and care as needed to correctly assemble the final cells.

3.1.7.1 Final Cell Assembly Problem Statement

DSSCs (including the cells used in this project) continue to be plagued by sealing issues. Cells produce leaks in a random manner. Solaronix AN-50 electrolyte is an extremely viscous and volatile liquid, making it difficult to contain. As discussed in the literature review, electrolyte containment and replacement alternatives are the emphasis of present work on DSSC technology.

3.1.7.2 Original Procedure

The DSSCs were originally assembled using binder clips. The procedure began by removing the working electrodes from the dye-solution. Heat resistant Kapton[®] tape was then placed over a strip of the conductive layer on both the working and counter electrodes. One last piece of Kapton[®] tape was placed on the top-center most, narrow portion of the sealant. The sealant was then secured on the working electrode by pressing the Kapton[®] tapes together; making sure the opening of the sealant was entirely within the TiO₂ active area.

The next step involved holding the working electrode with the attached sealant in the left hand and aligning the counter electrodes active area with the working electrodes. A binder clip was placed on the edge of one half of the cell. The cell would then be flipped over while still secured. This required agility and often resulted in misaligned working electrode and counter electrode active areas. The second binder clip was then placed on the opposite side of the cell. An assembled DSSC is shown in Figure 3.33.

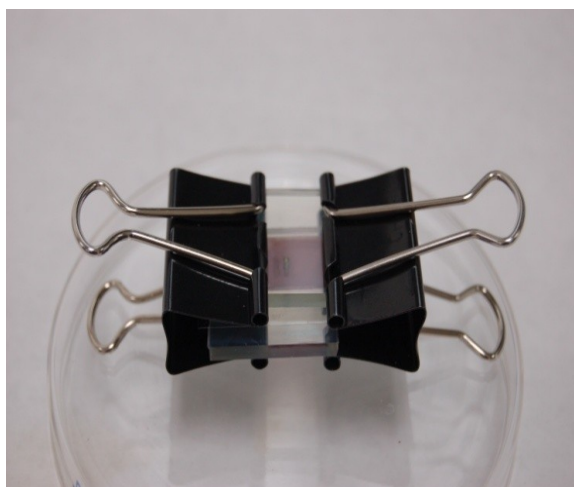


Figure 3.33: Original solar cell assembly technique

Once the binder clips were in position, the cell was placed on a Petri dish and heated in the furnace at 135°C for fourteen minutes to melt the sealant together with the working and counter electrodes. The cell was then removed from the furnace.

Electrolyte was inserted into a syringe and forcefully injected into the cavity on the counter electrode. Electrolyte injections were repeated up to three times on the same cell. The excess electrolyte was then cleaned off of the top of the cell. The cavity was sealed with low temperature hot glue. The cell would then be labeled and placed in a Petri dish for storage.

3.1.7.3 Steps Taken to Improve Methodology

Noticeable improvements had to be made for injecting the electrolyte and sealing the cell. Those two procedure steps relied too heavily on manual skills, which took months to acquire.

First iterations of improvements on the final assembly process began with searching for a way of aligning the active areas without picking up the cell. Devices are available that work by mechanically assembling the cells while applying heat; but those devices lie beyond this project's budget.

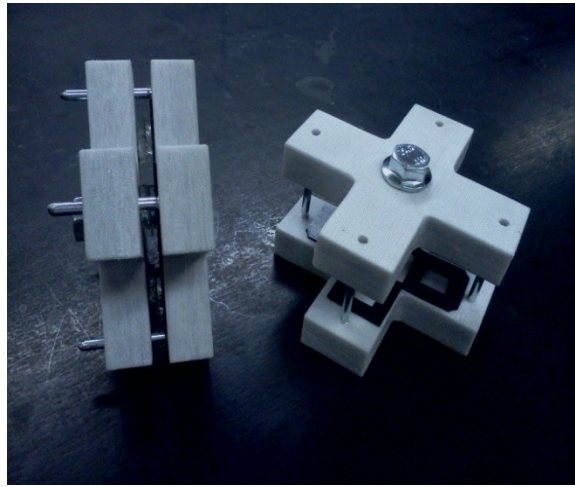


Figure 3.34: DSSC assembly presses

Two custom assembly presses (Figure 3.34) were designed and fabricated out of Teflon[®] woven CIP 300[®] grade plastic specifically for the final assembly process. Applied Plastics Machining manufactured the two presses with tight tolerances using designs supplied through SolidWorks[®] 2012 drawings (Figure 3.35).

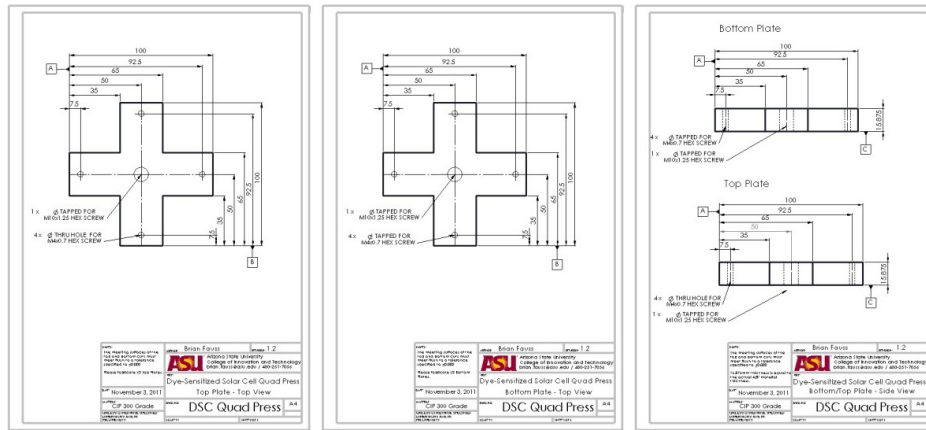


Figure 3.35: SolidWorks® 2012 drawings of assembly presses

Aluminum and steel were first considered before CIP 300®.

However, heat conducting materials such as metal would draw heat away from the cells, which would impact melting times and heat dissipation. The cells required even heat dispersion to the sealant from all sides of the cell to create a uniform melt. The material of the press was a good heat insulator.

The modified procedure started by removing the working electrodes from the dye-solution and allowing the ethanol a few minutes to completely evaporate from the electrodes. Kapton® tape was used to protect a conductive strip of the working and active electrodes. A working electrode was then secured between heat resistant foam on each branch of the press. A previously cut 60 um sealant was secured over the working electrode with a small piece of Kapton® tape. Next, a counter electrode was centered over the sealant by aligning the active areas of the electrodes (Figure 3.36). The top portion of the press could now be guided

down the posts and tightened in position. Applying a torque of 9.5 inch pounds to the central bolt using a torque wrench accomplished the task.

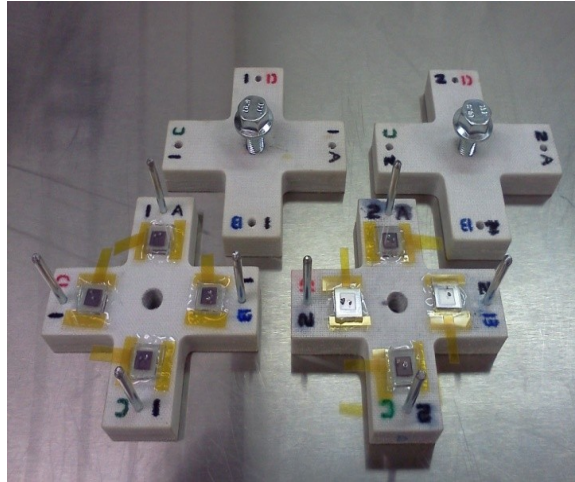


Figure 3.36: DSSC presses in use

The entire press was placed in the furnace at 135°C for fourteen minutes. The press was then removed from the furnace and allowed to cool for five minutes. A syringe needle was used to inject the electrolyte. All but 3 mm of the syringes' needle was clipped off to reduce damage to the TiO₂ layer during the electrolyte injection. The cells were then injected with electrolyte and sealed the same manner as the original procedure.

The presses worked well for a couple months, but then began producing two leaked cells per assembly procedure. The surface flatness had changed. CIP 300[®] plastic is heat resistant to 200°C, but gradually lost structural integrity over six months of use in 135°C temperatures. The presses were no longer dependable.

A different technique involving a hot plate was then explored. DSSCs could be assembled the same way as with the presses, but now in a Petri dish instead. The Petri dish containing an assembled but non-melted sealant was placed on a hot plate set at 115°C for three minutes, or until the sealant changed colors from light gray to transparent. During the color transition, firm pressure was applied to the top of the cell for five to ten seconds. Electrolyte injection and sealing were still performed the same way as in the previous assembly methods. After allowing the glue to dry for a few minutes, the cell was labeled with an ultra fine permanent marker. The cells were then stored in individual plastic containers within a larger plastic box. The cells were not disturbed for one to two days to allow the glue to harden and the electrolyte to penetrate into the TiO₂ pores for full cell activation.

3.2 Project Improvements

3.2.1 Lean Manufacturing

Lean manufacturing's 5S was applied to the entire project to improve workflow efficiency. For the purpose of this project, the 5S (1. *sorting* equipment and rearranging work stations; 2. *straightening* out tools and inventory; 3. *cleaning/sweeping* work area; 4. *standardizing* tool locations; and 5. *sustaining* the practice) methodology of Lean Manufacturing was used to reduce waste by applying the five components of the methodology.

A controlled work area was established by utilizing a more efficient workstation in an isolated area of the building. Four polished stainless steel workbenches were obtained from a decommissioned clean room. The benches were positioned to allow three researchers to function independently but effectively as a team. After this modification, the stations were located closer to frequently used equipment such as the coating machine, microscope, and high speed drill.

The supplies on the top two shelves of the storage locker were sorted and cleaned. Active materials were transferred to airtight containers to minimize accelerated degradation and contamination. Those materials include titanium dioxide paste, platinum solution, dye and electrolyte. Seldom-used items were either discarded if unusable or reorganized and relocated to lower shelves. This organization provided additional space for frequently used materials and tools, which permitted ready access to them for more effective and efficient use.

3.2.2 Solar Testing Station

Performance testing is not included within the scope of the fabrication process; however, performance testing must be improved to enable standardized testing of cells following the fabrication process. The three-component performance testing station includes a class III solar simulator, an electro-chemical machine, and a desktop computer. International testing standards are applied to solar cell testing stations so

that results can be shared and referenced in standard terms. Lack of compliance to standards is a significant problem. Prior to benchmarking the initial fabrication process, improvement must be instituted to comply with standard test conditions (STCs).

3.2.2.1 Solar Testing Station Problem Statement

Testing standards were not taken into account during the previous testing procedures. Another problem was that the formula used within Microsoft® Excel to interpret and calculate cell conversion efficiency was not labeled and the variables did not reflect testing standards. One physical problem was that the alligator clip's teeth damaged the conductive layer on the DSSCs.

3.2.2.2 Original Procedure

Prior to improvements made to the testing process, the procedure was to attach the electro-chemical machines leads using alligator clips to the anode and cathode of a fabricated DSSC. The DSSC was then placed on a platform directly below the solar simulators path of luminance. Next, the operator turned on the power to the three devices and pressed "Cell Enable" on the electro-chemical machine. Software on the computer was used to collect data and control the electrochemical machine. To obtain an I-V curve, the operator turned on the solar simulator light, and then clicked the "Start" button on PowerSuite™. The testing station's settings included:

1. solar simulator power output set to 135 W;
2. irradiance of 495 W/m²;
- 3.

the adjustable platform set at a height of 115 mm and; 4. the electrochemical machine set to drop voltages in one-second step increments. Once the I-V curve was completed, the raw data was saved to the computer's internal storage.

3.2.2.3 Steps Taken to Improve Methodology

Standard Test Conditions (STCs) is a universally accepted standard for solar testing and was chosen as the standard to implement. These testing conditions include the following variables: 1. irradiance of $1,000 \text{ W/m}^2$ (1 SUN); 2. Air Mass of 1.5 (AM1.5); and 3. ambient cell temperature of 25°C .

First, the irradiance on the platform from the solar simulator had to be corrected to $1,000 \text{ W/m}^2$. This was accomplished by calibrating an irradiance meter with a reference cell at a local photovoltaic testing laboratory. The original 9 V battery powering the irradiance meter gave false readings and so was replaced. The irradiance meter was now set to a height of 117 mm off the surface directly below the path of the solar simulator's light. Air Mass 1.5 is a solar angle of 48.2° away from Air Mass 0 (AM0), which gives an average irradiance of $1,000 \text{ W/m}^2$ at sea level. Solar simulators irradiate directly overhead at AM0 but rectify by matching an AM1.5 irradiance of $1,000 \text{ W/m}^2$. The power of the simulator was adjusted to 152 W, producing $1,000 \text{ W/m}^2$ on the readout of the irradiance meter. This resolved the irradiance and air mass conditions.

The ambient cell temperature was the next test condition to be corrected. Creating a heat transfer model and then physically testing the experiment to gauge the accuracy of the model predicted the surrounding and internal cell temperatures. In only three minutes and ten seconds under constant irradiance, cell temperatures rose to 7°C above STC temperatures. Room temperatures may vary a few degrees from 25°C, but are generally constant. A fan, blown on high speed was introduced to the testing station to reduce convective heating and keeping the tested cells from reaching temperatures greater than 30°C. Moving the testing station to a cooler room was considered, but the electrochemical machine is frequently used for other projects in the shared laboratory.

The electrochemical machine's step times were decreased to 0.065 seconds in order to collect I-V curves in less time. This reduced the amount of time the cell had to be under irradiance and heat. It was later observed that increasing the step time to these extremes produced undesirable effects on the I-V curve shape. This produced inaccurate efficiencies due to an altered Fill Factor (FF). The testing station was reverted back to one-second step times to rectify this adverse effect.



Figure 3.37: Mounted testing station

The testing stations' simulator lamp and adjustable platform was secured with brackets and bolts to ensure that all parameters remained unaltered (Figure 3.37 above). Now that STC was achieved, a Microsoft® Excel file was created to incorporate the new variables. The solar conversion efficiency equation is presented below. For this project, irradiance on the DSSC and the active cell area are constants in the equation below. The irradiance is $1,000 \text{ W/m}^2$, and active cell area is $38.44 \times 10^{-6} \text{ m}^2$.

$$\text{Efficiency } (\eta) = \frac{\text{Output} \times \text{Fill Factor}}{\text{Input}} \times 100 = \frac{(I_{sc} \times V_{oc}) \times \left(\frac{I_{mp} \times V_{mp}}{I_{sc} \times V_{oc}}\right)}{\text{Irradiance} \times \text{Cell Area}} \times 100$$

The last remaining issue to address was the damage to the conductive FTO layers caused by the abrasive alligator clip teeth. A newly designed jig was created and mounted to hold the cells without damaging the layers (Figure 3.38). The jig originally worked effectively with 3.0 mm thick glass substrate cells, but had negative impact on the cells created

from 2.3 mm thick glass. The pressure proved too great on the thinner glass cells, which pried a majority of them apart or enough to allow the electrolyte to leak. The jig was removed from the platform when 3.0 mm thick substrates were phased out of the project. A solution to the abrasive alligator teeth still remains unresolved.

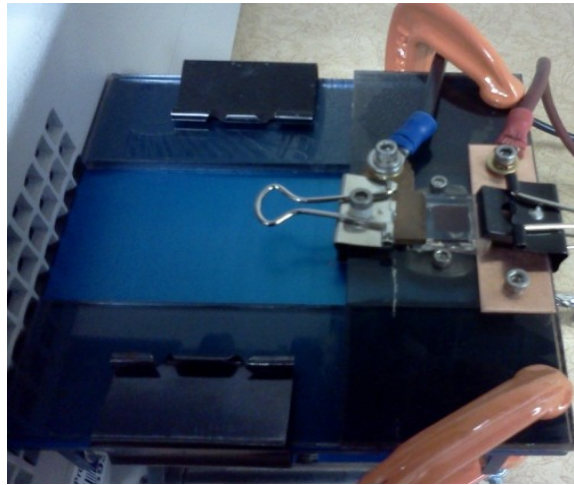


Figure 3.38: Photograph of testing jig on platform

Black electrical tape was now added to the platform (Figure 3.39) to reduce reflection from the platform's surface as well as serving as an electrical insulator. There was potential for the conductive metal of the platform to create a short circuit between the alligator clips, which would alter testing results.

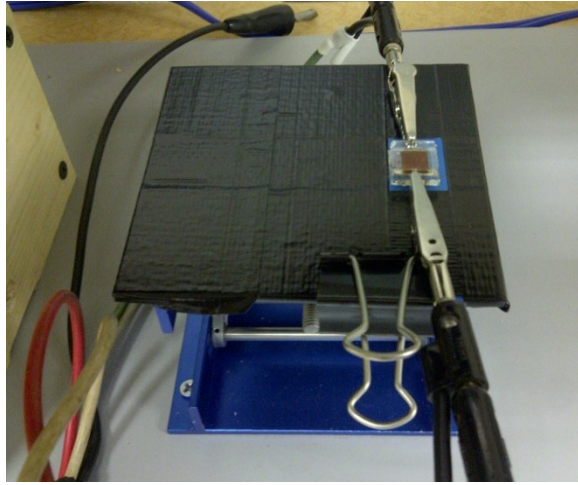


Figure 3.39: Testing platform setup

Chapter 4

RESULTS AND DISCUSSION

4.1 Fabrication Improvements

4.1.1 Titanium Dioxide Deposition

The titanium dioxide deposition process was the bottleneck of the DSSC project. It is critical to develop a process to achieve consistently uniform TiO₂ layers, for successful fabrication of working DSSCs. However, the cells frequently failed during final assembly procedures when the TiO₂ layers were not uniform. The original process began on the coating machine using a glass rod attached to the mechanical armature. A subsequent improvement was made with the introduction of the steel doctor blade armature attachment. However, both of the initial techniques had problems involving large variation in the thickness and uniformity of the coating. At this juncture, this study employed Six Sigma's DMAIC to rectify these problems. Through several iterations of DMAIC cycles, improvements were made, which brought control to the titanium dioxide deposition process.

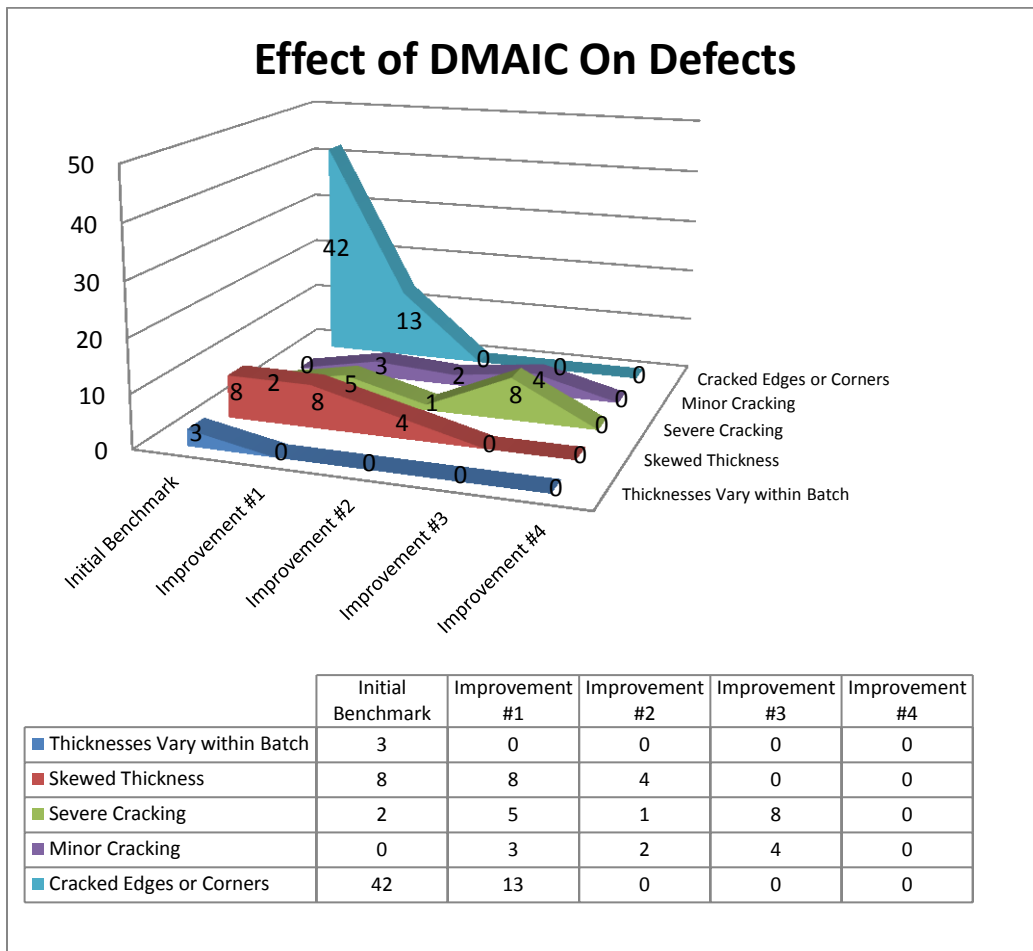


Figure 4.1: Effect of DMAIC on defects during the TiO₂ deposition process

Figure 4.1 above illustrates the progress of using DMAIC to reduce defects during the titanium dioxide deposition process. The first benchmark represents the initial process. The other benchmarks are points in time where modifications were implemented to the TiO₂ deposition process.

Inputting the defects and opportunities for defects into the iSixSigma[®] process Sigma calculator (Table 4.1 below) showed that the process Sigma value increased as modifications were made. Z-score and

process sigma are the same. The Z-score represents the process performance. The positive infinite z-score in the “Process Sigma” column means that the current process gives us a one hundred percent yield of products. In other words, there are no measurement boundaries because there were no defects to set the limits.

	Defects	Opportunities for Defects	Defects per Million Opportunities	Process Sigma (Z score)
Benchmark #1	55	280	196429	2.35
Benchmark #2	29	120	241667	2.20
Benchmark #3	7	40	175000	2.43
Benchmark #4	12	220	54545	3.10
Benchmark #5	0	100	0	+ ∞ Z

Table 4.1: Titanium Dioxide Deposition Process Sigma

Table 4.2 below shows that the procedure time and amount of defects were significantly reduced after completing the process improvements. The procedure time was decreased to twenty-eight minutes and thirty seconds from the original time of one hour and twelve minutes. Additionally, the amount of defects drastically decreased after modifications. The amount of ideal TiO₂ layers increased from twenty-three percent to one hundred percent.

	Weekly Process Time	Weekly Procedure Time	Defect-Free TiO ₂ Layers
Initial Process	2:57:00	1:12:00	13 of 56
Final Improved Process	2:13:30	0:28:30	20 of 20
Difference	0:43:30	0:43:30	
Percent Improvement	33 %	153 %	331 %

Table 4.2: Titanium Dioxide Deposition improvements in process and procedure times

4.1.2 Dye Solution Preparation

Utilizing sterilized sealing jars for preparing and storing the dye solution saved time and material. The original sub-process involved the use of an extra mixing container and wax paper covering. Dye and ethanol were wasted because the Petri dish volume was excessive for soaking four working electrodes. Dye and ethanol was also wasted because the wax paper did not properly seal the Petri dish. The dye solution sub-process took about twenty-five minutes to complete every other week.

Using sealed jars eliminated the need for wax paper and transferring of containers. Instead of discarding the solution because of settling dye particles, the entire jar can now be placed directly in the ultrasonic stirring bath. The procedure does not need to be frequently repeated and is reduced to a one-time fifteen minutes procedure. Weekly time savings can be seen in Table 4.3 below. After nearly three months, the sealed jars containing the dye solution were still usable.

	Weekly Procedure Time
Original Process	0:12:30
Modified Process	0:01:22
Difference	0:11:08
Percent of Improvement	815 %

Table 4.3: Improvement in dye solution preparation time

4.1.3 Glass Cutting

Procedure times are significantly decreased after modifying the cutting procedure by means of a new template, laser cutting files and settings. The original process took forty-five minutes to cut each 5 cm x 5 cm sheet of glass. For each sheet of glass, only forty-four percent was usable after cutting. This meant the cutting process had to be repeated weekly to produce the required weekly minimum of six usable substrates.

After modifying the process, one hundred percent of the cut glass substrates are usable (Table 4.4). The new procedure requires only five minutes and thirty seconds per sheet and glass now only has to be cut once every three weeks because of the high success rate. This results in glass cutting times of one minute and fifty seconds per week. The revised process also insures that there is no damage to the glass conductive FTO layer. Before and after modification results are displayed in Table 4.4 below.

	Weekly Procedure Time	Usable Substrates
Original Process	0:45:00	7 of 16
Modified Process	0:01:50	16 of 16
Difference	0:43:10	9 of 16
Percent Improvement	2,354 %	129 %

Table 4.4: Improvements in glass cutting procedure time and success rate

4.1.4 Glass Drilling

Improvements from modifying the glass drilling process resulted in less defective substrates and decreased procedural time. The original drilling process intermittently damaged conductive FTO layers, cracked glass pieces, and produced misaligned cavities. Six substrates were defective out of eighteen drilled, resulting in a sixty-seven percent success rate. The original process took roughly five minutes per drilled substrate.

The modified drilling process resulted in only three defective substrates out of twenty (Table 4.5). One substrate cracked and two drill bits broke inside of two other substrates. The process success rate improved to eighty-five percent with no additional damage to the conductive FTO layers. The process time was reduced to one minute and forty seconds per substrate (Table 4.5).

	Weekly Procedure Time	Usable Substrates
Original Process	0:15:00	12 of 18
Modified Process	0:05:00	17 of 20
Difference	0:10:00	
Percent of Improvement	200 %	28 %

Table 4.5: Improvements in glass drilling procedure time and success rate

Two additional modifications in the glass drilling process resulted in tangible benefits. Improved placement of the drilled cavities also helped make the electrolyte injection more consistent during the final assembly process. The reduced drill bit size greatly benefited the platinum deposition process.

4.1.5 Platinum Deposition

Platinum layers were deposited using the same doctor blade technique as used in the original process but had entirely different results due to the modifications made during the glass drilling sub-process. The platinum coat applied uniformly once the funneling effect was eliminated by means of the reduced drilled cavity size. Improvements in to the coating mask procedure of the process allowed for consistent placement of the platinum layer, which proved valuable during the final assembly process.

The coating mask originally took four minutes to make but time was reduced to thirty seconds in the modified procedure. Process duration improved slightly from two hours to one hour and fifty-six minutes.

However, one hour and forty-five minutes of the process duration was sintering time in the furnace. The physical procedure time was reduced from fifteen minutes to eleven minutes per week (Table 4.6). The greatest benefit to this process was not realized in time savings, but rather in improved consistency and placement of the platinum layer.

	Weekly Process Time	Weekly Procedure Time
Original Process	2:00:00	0:15:00
Modified Process	1:56:00	0:11:00
Difference	0:04:00	0:04:00
Percent of Improvement	5 %	36 %

Table 4.6: Improvements in platinum deposition process and procedure times

4.1.6 Sealant Preparation

Original sealant cutting procedures involved cutting estimated-sized outside sealant borders with scissors and an inside border area with an X-Acto[®] utility blade. The sealant size dimensions were rarely consistent and the inside borders were not entirely straight.

The modified process utilized a paper cutter for making consistent 16 mm outside border areas and a flat X-Acto[®] chisel blade for each edge of the inner area of the sealant. The modifications eliminated variation in sealant sizes and also reduced the procedure time. The cutting process was decreased to a minute and fifteen seconds per sealant with uniformly

cut dimensions, versus a previous time of three minutes per sealant. The amount of weekly savings in procedure time is given in Table 4.7 below.

	Weekly Procedure Time
Original Process	0:09:00
Modified Process	0:03:45
Difference	0:05:15
Percent of Improvement	140 %

Table 4.7: Sealant preparation improvement in preparation time

4.1.7 Final Assembly

DSSC assembly has been challenging. The original assembly procedure relied heavily on the manual skills and patience of the assembler. Two assembly jigs were created to instill consistency, but they did not hold up to long-term use under high temperatures. The most recent modification revision involving assembly on a hot plate is not perfect but generally works well.

Process control of the other processes and sub-process largely determined the success rate of the final assembly process. The success rate during final assembly was determined by the amount of cells that functioned with efficiencies greater than five percent. A five percent minimum target was deemed reasonable since defect free cells showed efficiencies between five and one half to ten and one half percent.

Only two out of the first twelve cells (seventeen percent) were assembled without defects. Following modifications to all of the processes

and sub-processes, the success rate rose to ninety percent. Eighteen out of twenty cells were assembled defect free. Even though the procedures changed, the final assembly procedure times did not. The original final assembly process and improved final assembly process both required fifteen minutes for each cell. Table 4.8 shows that the quantity of functioning cells greatly improved while assembly time did not. It was not determinable whether the cause of cells not functioning occurred due to assembly errors or to faulty individual components.

	Weekly Procedure Time	Functioning Cells
Original Process	0:45:00	2 of 12
Modified Process	0:45:00	18 of 20
Difference	0:00:00	
Percent of Improvement	0 %	440 %

Table 4.8: Improvements in final assembly process and procedure times

4.2 Project Improvements

4.2.1 Lean Manufacturing

Implementing the 5S methodology on this project increased production efficiency. DSSCs are now made more accurately in less time than with previous methods. Modifications made using 5S methods resulted in the following improvements:

- Faster access to tools and equipment.
- Better environment for reducing foreign contamination.

- Cooler ambient temperatures - better suited for preserving materials.
- Tools and equipment only require cleaning prior to each procedure rather than continually throughout the procedure.

These improvements from using 5S methods greatly simplified procedural tasks. The results listed above are consistent with what can be expected according to literature on Lean Manufacturing benefits [65]. Benefits from adopting 5S methods are absorbed into each individual process. Lean Manufacturing results are not as quantifiable as Six Sigma's results.

Figure 4.2 shows the comprehensive fabrication process that was optimized to be completed in three days rather than in five days. The original process was performed inconsistently throughout a span of five days.

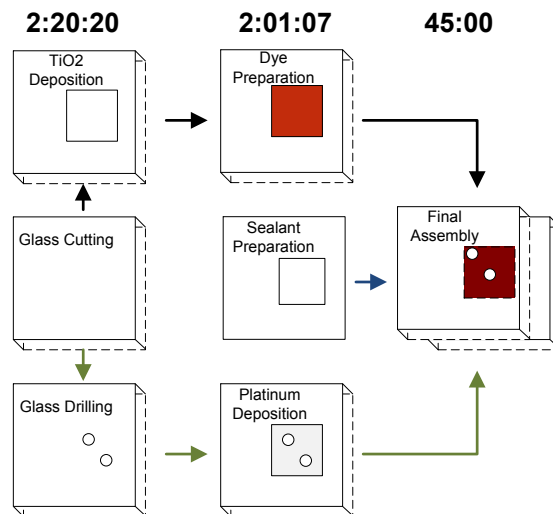


Figure 4.2: Optimized DSSC fabrication flow chart

4.2.2 Solar Testing Station

The testing station is now mounted in a fixed position and calibrated for STC at 1 Sun. The improved setup reduced variation in readings caused by inconsistent positioning. DSSC exposure time under illumination was reduced by more than half. Two different step times are incorporated into the modified process, which allows cell measurements in only two minutes and fifteen seconds per cell. With the previous method, the cells were under constant illumination for three tests each of which took one minute and forty-five seconds to complete, for a total test time of five minutes and fifteen seconds. Table 4.9 below compares times for measuring three cells three times a week.

	Weekly Procedure Time
Original Process	0:42:15
Modified Process	0:20:15
Difference	0:22:00
Percent Improvement	109 %

Table 4.9: Comparison of time to test original and modified process on three cells, three times per week

Prolonged cell exposure to illumination increased the cell temperature, which altered the I-V curve characteristics. The resulting raise in ambient temperatures above from 25°C also removed the test from conformity to STC standards.

The alligator clip teeth continue to scratch the conductive film of the glass. Damaged electrode conductive films will ultimately affect long-term measuring accuracy. This problem must be resolved by finding a better type of clamp.

4.3 Combined Results

Each individual process and sub-process and the supporting project processes were modified. All key components of the project were improved. Lean Manufacturing's 5S methods contributed to reduced procedure times. The total amount of weekly time spent actively fabricating the DSSCs was reduced from four hours and fifteen minutes to an hour and fifty-six minutes. These are considered the procedural times. However, for the purposes of process control and optimization, the entire process time is significant to gauging improvement.

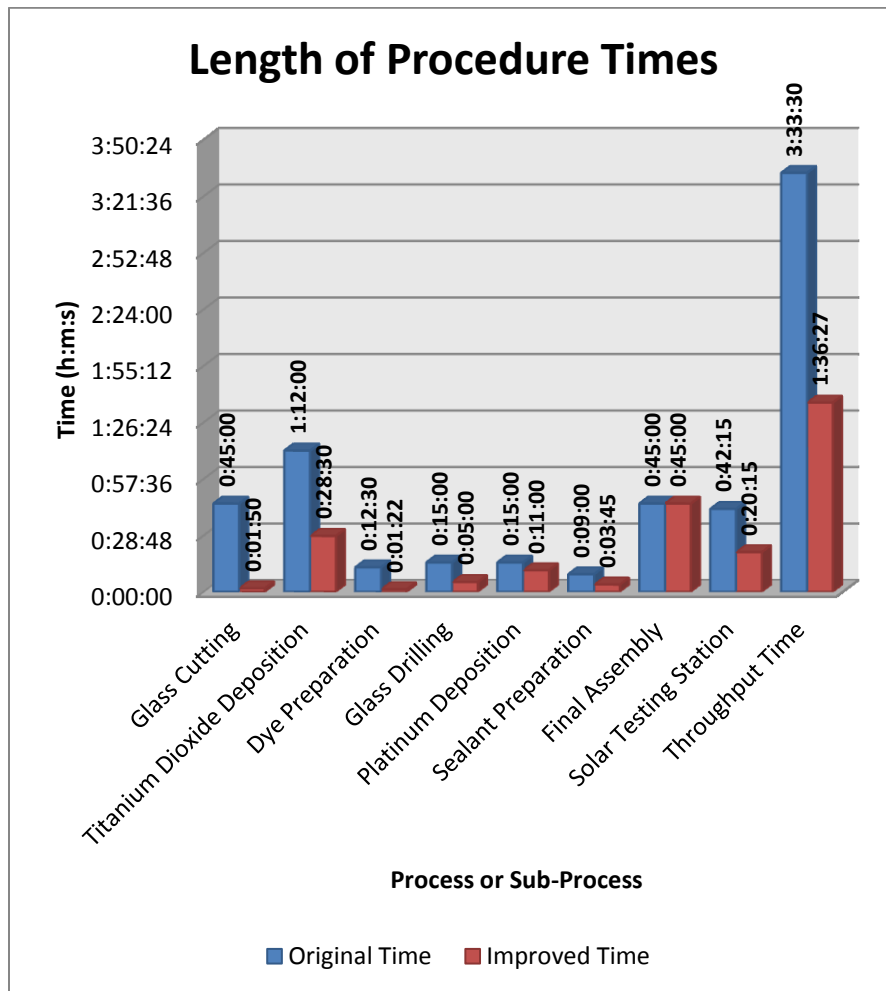


Figure 4.3: Amount of time required to complete procedures

Procedures are steps taken to accomplish each process. Figure 4.3 shows the amount of time weekly it takes to complete individual processes. The “TOTALS” column shows the entire amount of time it takes to make three DSSCs per week. The titanium dioxide deposition and platinum deposition processes each include an extra hour and forty-five minutes for sintering each week. This is standby time, which is part of the processes but not included in procedural time.

Chapter 5

CONCLUSIONS

5.1 Overview

Originally, the DSSC experiment operated in a satisfactory manner. Results often ranged from good to excellent, if the cells functioned properly. However, the length of fabrication time and the consistency between produced DSSC samples were by no means optimal.

This project improved the DSSC fabrication process by using methods and tools learned in various ASU courses, including: energy transfer modeling, statistical process control, quality assurance, Lean Six Sigma Green Belt certification, reliability and standards, applied photovoltaics, solar cells, and evaluation of photovoltaics.

An analytical problem-solving approach was taken to modify and improve this DSSC project. The original DSSC project contained eight processes; it was the goal of this research to measure and improve efficiency in each of the eight areas. This study demonstrated that several improvement methods could be used to eliminate multiple defects and reduce procedural times throughout each of the eight processes. Several methods were introduced to identify and significantly reduce the root causes of defects and to optimize each of the individual procedures included within the scope of the project. These methods included: Lean Manufacturing's 5S, Six Sigma's DMAIC, thermal energy modeling, and

standardization using standard test conditions and a standard operating procedure.

Table 5.1 shows how Lean Manufacturing’s 5S method was used as a catalyst to enhance procedural times, therefore, improving the project performance efficiencies. The amount of time to produce a batch of cells was reduced from five days to three. Combined weekly procedural times were dramatically decreased by 119 %.

	Weekly Procedural Time (Efficiency)	Reduction of Defects within Process (Effectiveness)
Glass Cutting	2,354	129
Dye Solution Preparation	815	-
Glass Drilling	200	28
TiO ₂ Deposition	153	331
Sealant Preparation	140	-
Solar Testing Station	52	-
Platinum Deposition	36	-
Final Cell Assembly	0	440

Table 5.1: Percent improvement of procedural times and percent reduction of defects within each process

Six Sigma’s DMAIC methodology proved valuable as demonstrated on the titanium dioxide deposition process of this project. All defects, including the previously unknown causes of defects were identified and eliminated. By systematically improving each individual process, the effectiveness of fabricating the DSSC’s was increased by an impressive

440 %. This effectiveness improvement calculation was based on the number of cells that functioned above 5 % conversion efficiency after assembly.

In addition to the improvements achieved, an SOP was created to standardize the procedures to help ensure that other researchers without losing efficiency or effectiveness can continue the fabrication process.

Benefits of improving the efficiency and effectiveness of the project have been to: significantly reduce fabrication and rework time, reduce waste of materials and associated costs, plus to introduce much needed process control.

This experiment demonstrated that using a methodical approach to problem solving could not only result in substantial improvements in efficiency and effectiveness, but also enhance the reliability and quality of the study.

5.2 Future Recommendations

Research involving low cost alternatives to platinum in the counter electrode is a promising topic for study. Carbon composites have been found to be more cost effective, while outperforming platinum. Different forms of carbon nanotubes are also being explored as an alternative conductor. Carbon nanotubes provide excellent electron conduction properties. Prices continue to decrease, making nanotubes a viable platinum replacement option.

DSSC reliability is hindered by the lack of containment of the viscous electrolyte. Research opportunities exist in regards to finding alternate sealing methods to those currently practiced.

Further research is also needed in DSSC testing standards and testing conditions. Unlike silicon solar cells, DSSCs are electro-chemical solar cells, which behave inconsistently under standard test conditions. Research is needed to create a more accurate standardized test condition for DSSCs. Testing step rates and time under irradiance drastically influences I-V curve characteristics. The impact on cell performance is not well documented.

REFERENCES

- [1] K. Kinhal, "Effects Of Sputtered Platinum Counter Electrode And Integrated TiO₂ Electrode With SWCNT On DSSC Performance," ProQuest LLC, Ann Arbor, 2011.
- [2] A. R. Jha, *Solar Cell Technology And Applications*, New York: CRC Press, 2009.
- [3] S. Schweikhart, "The Applicability Of Lean And Six Sigma Techniques To Clinical And Translational Research," *Journal of Investigative Medicine*, vol. 57, no. 7, p. 748, 2009.
- [4] A. G. Psychogios, "Lean Six Sigma In A Service Context," *The International Journal of Quality & Reliability Management*, vol. 29, no. 1, p. 122, 2012.
- [5] T. Tran, *Implementation Of Lean Six Sigma Principles In An Analytical Research And Development Chemistry Laboratory At A Medical Device Company*, Ann Arbor: ProQuest LLC, 2011.
- [6] C. Delgado, "The Implementation Of Lean Six Sigma In Financial Services Organizations," *Journal of Manufacturing Technology Management*, vol. 21, no. 4, p. 512, 210.
- [7] B. Elder, "Six Sigma In The Microbiology Laboratory," *Clinical Microbiology Newsletter*, vol. 30, no. 19, p. 143, 2008.
- [8] A. Johnson and B. Swisher, "How Six Sigma Improves R&D," *Research Technology Management*, vol. 46, no. 2, p. 12, 2003.
- [9] J. Antony, "Six Sigma vs Lean: Some Perspectives From Leading Academics And Practitioners," *International Journal of Productivity and Performance Management*, vol. 60, no. 2, pp. 185-190, 2011.
- [10] E. A. A. V. V. John Maleyeff, "The Continuing Evolution Of Lean Six Sigma," *The TQM Journal*, vol. 24, no. 6, pp. 542 - 555, 2012.
- [11] U.S. Energy Information Administration, "Annual Energy Review 2011," Department of Energy, District of Columbia, 2012.
- [12] D. Levitan, "The Solar Efficiency Gap," *IEEE Spectrum*, pp. 11-12, June 2012.

- [13] S. Wenham, M. Green, M. Watt and R. Corkish, "Chapter2: Semiconductors And P-N Junctions," in *Applied Photovoltaics*, London, Earthscan, 2007, pp. 31-38.
- [14] N. C. f. Photovoltaics, Artist, *Best Research-Cell Efficiencies*. [Art]. National Renewable Energy Laboratories, 2012.
- [15] R. King, "Solar Cell Generations Over 40% Efficiency," *Progress in Photovoltaics: Research and Applications*, no. 20, pp. 801-815, 2012.
- [16] A. Hinsch, "Worldwide First Fully Up-Scaled Fabrication Of 60 × 100 cm² Dye Solar Module," *Progress in Photovoltaics: Research and Applications*, vol. 20, no. 6, p. 698–710, 2012.
- [17] J. Reid, "G24 Innovations Ships World's First Commercial Application Of DSSC Solar Technology," *Business Wire*, New York, 2012.
- [18] Y. Chiba, A. Islam, Y. Watanabe, R. Komiya, N. Koide and L. Han, "Dye-Sensitized Solar Cells With Conversion Efficiencies Of 11.1%," *Japanese Journal of Applied Physics*, vol. 45, pp. 638-640, 2006.
- [19] B. O'Regan and M. Gratzel, "A Low-Cost, High-Efficiency Solar Cell Based On Dye-Sensitized Colloidal TiO₂ Films," *Nature*, vol. 353, no. 6346, pp. 737-740, 1991.
- [20] A. Yella, "Porphyrin-Sensitized Solar Cells With Cobalt (II/III)–Based Redox Electrolyte Exceed 12 Percent Efficiency," *Science Magazine*, pp. 629-634, 4 November 2011.
- [21] J. Moser, *Monatsh Chem*, vol. 8, p. 373, 1887.
- [22] H. Gerischer and H. Tributsch, *Berich Buns Gesell*, vol. 72, p. 437, 1968.
- [23] H. Tributsch and H. Gerischer, *Berich Buns Gesell*, vol. 73, p. 251, 1969.
- [24] H. Gerischer, H. Schoppel and B. Pettinge, *Journal of Electrochemistry Society*, vol. 119, p. C230, 1972.
- [25] R. Memming, "Photochemical Processes In Monomolecular Dye Layers On SnO₂," *Faraday Discussions*, vol. 58, pp. 261-270, 1974.

- [26] R. Memming and F. Schröppel, "Electron Transfer Reactions Of Excited Ruthenium(II) Complexes In Monolayer Assemblies At The SnO₂-Water Interface," *Chemical Physics Letters*, vol. 62, no. 2, pp. 207-210, 1979.
- [27] R. Memming, F. Schroppel and U. Bringmann, *Journal of Electrochemical Chemistry*, vol. 100, pp. 307-318, 1979.
- [28] R. Faccio, "Current Trends In Materials For Dye Sensitized Solar Cells," *Recent Patents on Nanotechnology*, pp. 46-61, 2011.
- [29] M. Grätzel, "Dye-Sensitized Solar Cells," *Journal of Photochemistry and Photobiology*, vol. 4, p. 145–153, 2003.
- [30] O. Kohle, M. Gratzel, A. Meyer and T. Meyer, "The Photovoltaic Stability Of bis(isothiocyanato)Ruthenium(II)-bis-2,2'-Bipyridine-4,4'-Dicarboxylic Acid And Related Sensitizers," *Advanced Materials*, vol. 9, no. 11, p. 904, 1997.
- [31] K. Murakoshi, G. Kano, Y. Wada, S. Yanagida, H. Miyazaki, M. Matsumoto and S. Murasawa, "Importance Of Binding States Between Photosensitizing Molecules And The TiO₂ Surface For Efficiency In A Dye-Sensitized Solar-Cell," *Journal of Electroanalytical Chemistry*, vol. 396, no. 1, pp. 27-34, 1995.
- [32] K. Murakoshi, R. Kogure, Y. Wada and S. Yanagida, "Solid State Dye-Sensitized TiO₂ Solar Cell With Polypyrrole As Hole Transport Layer," *Chemistry Letters*, no. 5, pp. 471-472, 1997.
- [33] G. O. ., P. C. S. Fei Cao, "A Solid State, Dye Sensitized Photoelectrochemical Cell," *Journal of Physical Chemistry*, vol. 99, no. 47, p. 17071–17073, 1995.
- [34] A. F. Nogueira and M.-A. De Paoli, "Electron Transfer Dynamics In Dye Sensitized Nanocrystalline Solar Cells Using A Polymer Electrolyte," *The Journal of Physical Chemistry B*, vol. 105, no. 31, p. 7517–7524, 2001.
- [35] W. Gazotti, A. Nogueira, E. Girotto, M. Gallazzi and M. De Paoli, "Flexible Photoelectrochemical Devices Based On Conducting Polymers," *Synthetic Metals*, vol. 108, no. 2, pp. 151-157, 2000.
- [36] W. Kubo, K. Murakoshi, T. Kitamura, Y. Wada, K. Hanabusa, H. Shirai and S. Yanagida, "Fabrication Of Quasi-Solid-State Dye-

Sensitized TiO₂ Solar Cells Using Low Molecular Weight Gelators," *Chemistry Letters*, pp. 1241 - 1242, 1998.

- [37] K. Tennakone, G. Kumara, I. Kottegoda, K. Wijayantha and V. Perera, "A Solid-State Photovoltaic Cell Sensitized With A Ruthenium Bipyridyl Complex," *Journal of Physics D: Applied Physics*, vol. 31, no. 12, pp. 1492-1496, 1998.
- [38] K. Tennakone, G. Kumara, A. Kumarasinghe, K. Wijayantha and P. Sirimanne, "A Dye-Sensitized Nano-Porous Solid-State Photovoltaic Cell," *Semiconductor Science and Technology*, vol. 10, no. 12, pp. 1689-1693, 1995.
- [39] K. Tennakone, G. Kumara, K. Wijayantha, I. Kottegoda, V. Perera and G. Aponso, "Nano-Porous Solid-State Photovoltaic Cell Sensitized With Tannin," *Semiconductor Science and Technology*, vol. 13, no. 1, pp. 134-138, 1998.
- [40] K. Tennakone, A. Kumarasinghe and P. Sirimanne, "Dye Sensitization Of Low-Bandgap Semiconductor Electrodes: Cuprous Oxide Photocathode Sensitized With Methyl Violet," *Semiconductor Science and Technology*, vol. 8, no. 8, pp. 1557-1560, 1993.
- [41] B. O'Regan and D. Schwartz, "Efficient Dye-Sensitized Charge Separation In A Wide-Band-Gap P-N Heterojunction," *Journal of Applied Physics*, vol. 80, no. 8, pp. 4749 - 4754, 1996.
- [42] B. O'Regan and D. Schwartz, "Large Enhancement In Photocurrent Efficiency Caused By UV Illumination Of The Dye-Sensitized Heterojunction TiO₂/RuLL'NCS/CuSCN: Initiation And Potential Mechanisms," *Chemistry of Materials*, vol. 10, no. 6, pp. 1501-1509, 1998.
- [43] A. Hicks, Artist, *Layered Components Of A DSSC*. [Art]. National Renewable Energy Laboratory, 2012.
- [44] Y. Lee, C. Chen, C. Chen, L. Chong, Y. Liu and C. Chi, "A Platinum Counter Electrode With High Electrochemical Activity And High Transparency For Dye-Sensitized Solar Cells," *Electrochemistry Communications*, vol. 12, no. 11, p. 1662-1665, 2010.
- [45] F. Li, L. Wang, S. Fu, Z. Huo and Y. Gu, "A Novel Improved Method To Increase The Efficiency Of Dye-Sensitized Solar Cells," *Journal of the Chinese Chemical Society*, vol. 58, no. 3, pp. 408-411, 2011.

- [46] World Energy Council, "2004 Survey Of Energy Resources," Oxford, 2004.
- [47] S. Lin and W. Chou, "Investigation Of Pentacene/Perylene Derivative Based Organic Solar Cells," National Cheng Kung University, Tainan Tawian, 2007.
- [48] V. Sterling, *Planning And Installing Photovoltaic Systems: A Guide For Installers*, London: James & James / Earthscan, 2008.
- [49] Solaronix, Artist, *Ruthenizer 535-bisTBA*. [Art]. Solaronix SA, 2012.
- [50] C. J. Barbe, "Nanocrystalline Titanium Oxide Electrodes For Photovoltaic Applications," *Journal of the American Ceramic Society*, vol. 80, no. 12, pp. 3157-3171, 1997.
- [51] G. Polesky, *Lean Six Sigma Process Improvement Certification*, Mesa: ASU, 2012.
- [52] J. Womack and D. Jones, *Lean Thinking: Banish Waste And Create Wealth In Your Corporation*, London: Simon and Schuster, 1996.
- [53] B. Franklin, "Poor Richard's Almanac And The Way To Wealth," *Writing*, vol. 25, no. 6, pp. 14-16, 2003.
- [54] P. Sterman, "Jack Welch Boosts Six Sigma," *OC Metro*, p. 60, 2005.
- [55] M. L. George, *Lean Six Sigma : Combining Six Sigma Quality With Lean Speed*, New York: McGraw-Hill, 2002.
- [56] M. Pepper and T. A. Spedding, "The Evolution Of Lean Six Sigma," *The International Journal of Quality & Reliability Management*, vol. 27, no. 2, pp. 138-155, 2010.
- [57] V. Kruger, "The Quality Gurus," *Measuring Business Excellence*, vol. 6, no. 3, pp. 57-58, 2002.
- [58] M. Kulis and Z. Mrduljas, "Quality Gurus," *Technicki Vjesnik-Technical Gazette*, vol. 16, pp. 71-78, 2009.
- [59] M. M. Helms, *Encyclopedia Of Management*, Detroit: Encyclopedia of Management, 2006.

- [60] X. Zhu, "Lean Six Sigma: A Literature Review," *Interdisciplinary Journal of Contemporary Research In Business*, vol. 3, no. 10, p. 599, 2012.
- [61] K. Robinson, "GLPs And The Importance Of Standard Operating Procedures," *Biopharm International*, no. 16, pp. 38-46, 2003.
- [62] J. Kallman, "Creating A Standard Operating Procedures Manual," *Risk Management*, no. 53, p. 42, 2006.
- [63] D. C. Peterson, "Assuring The Effective Use Of Standard Operating Procedures (SOPs) In Today's Workforce," *Biopharm International*, no. September, pp. 42-46, 2006.
- [64] A. K. Htun, *Characterization Of Dye-Sensitized Solar Cells With Different Nanoparticles*, Mesa, Arizona: Arizona State University, 2010.
- [65] R. W. Hoerl, "Lean Six Sigma, Creativity, and Innovation," *International Journal of Lean Six Sigma*, vol. 1, no. 1, p. 30, 2010.

APPENDIX A
STANDARD OPERATING PROCEDURE (SOP)

TABLE OF CONTENTS

1. SAFETY	
Laboratory Safety Equipment	1
Safety Concerns	1
2. ESTABLISHING FABRICATION SCHEDULE	
Contingency Planning	2
Material Timing Considerations	2
Schedule Example	2
3. CUTTING GLASS	
Materials/Equipment.....	3
Quantity.....	3
Procedure	3
4. PREPARING SEALANT	
Materials/Equipment.....	6
Quantity.....	6
Procedure	6
5. DRILLING COUNTER ELECTRODE	
Materials/Equipment.....	8
Quantity.....	8
Procedure	8
6. RUTHENIUM DYE SOLUTION PREPARATION	

Materials/Equipment.....	10
Quantity.....	10
Procedure	10
7. FABRICATING WORKING ELECTRODE	
Materials/Equipment.....	11
Quantity.....	11
Procedure	11
8. PREPARING COUNTER ELECTRODE	
Materials/Equipment.....	15
Quantity.....	15
Procedure	15
9. ASSEMBLING SOLAR CELL	
Materials/Equipment.....	19
Quantity.....	19
Procedure	19
10. MEASURING PERFORMANCE / DATA COLLECTING	
Materials	24
Procedure	24
I-V Curve Interpretations.....	25

1. SAFETY

1.1. Laboratory Safety Equipment – The operator must follow proper equipment operating procedures for each specific piece of equipment and wear protective gear as well as follow specific safety procedures for handling chemicals. To avoid harm the operator should use the following safety equipment:

- UV goggles to use the laser
- Hearing protection to drill
- UV goggles to use solar simulator
- Respiratory mask to laser cut polymers
- Lab safety glasses to handle chemicals
- White laboratory coat at all times
- Latex gloves at all times

1.2 Safety Concerns – The operator should refer to individual lab policies at all times.

2. ESTABLISHING FABRICATION SCHEDULE

2.1. Contingency Planning

2.1.1. When scheduling fabrication of cells, the researcher must incorporate buffers and backup plans in order to be prepared for unforeseen events. Examples of such events can include, but are not limited to: budget constraints, occupied equipment, depleted supplies, expired or ruined titanium dioxide or platinum materials, researchers inability to complete the cell batch (such as vacations, family emergencies, exams, lack of follow through by team members, etc.)

2.1.2. The preferred way of minimizing these project bottlenecks is to practice good communication and courtesy with other colleagues sharing the equipment, keeping a good back-stock of supplies by ordering materials well before they run out, and having a pre-established contingency plan for continuing a batch of cells in progress. This can be as simple as having a contact phone number of a colleague who can finish the batch of cells or properly store the unfinished cells until the batch can be completed.

2.2. Material Timing Considerations

2.2.1. *Titanium Dioxide*

2.2.1.1. Dry > 30 minutes after coated on glass

2.2.1.2. Place cells directly in dye-solution immediately after 12 hour sintering cool down period

2.2.2. *Platinum*

2.2.2.1. Dry > 5 minutes after coated on glass

2.2.2.2. Immediately use in assembly process following the 12 hour sintering cool down period

2.2.3. *Assembled Cells*

2.2.3.1. The electrolyte should be injected and the cells sealed > 30 minutes after assembly, but < 12 hours maximum lapsed time.

2.2.3.2. The completed cells must be left undisturbed for > 24 hours to allow the sealing agents to set before handling or measuring.

2.2.4. *Equipment*

2.2.4.1. Furnace – requires roughly 2 hours to cool down to room temperature with the furnace door left open

2.2.4.2. Hot Plate – takes about 5 minutes to warm up to 100°C

2.2.4.3. Hot Glue Gun – takes about 5 minutes to turn the glue stick into a usable gel

2.3. Schedule Example – This is an example of a planned schedule for fabricating cells every week.

July 2012

Sun	Mon	Tue	Wed	Thu	Fri	Sat
1 Material Prep	2 Measure Cells	3	4 Measure Cells	5 TiO ₂ Coating	6 Pt Coating Measure Cells	7 Assembly

3. CUTTING GLASS

3.1. Materials/Equipment

- 3.1.1. Fluorine Tin Oxide (FTO) coated Glass – 5cmx5cm Area, 2.2mm Thick, 7Ω/Sheet Resistance
- 3.1.2. Universal Laser Systems Cutting/Engraving Laser
- 3.1.3. 3M® Scotch® Low Tact Artist Tape
- 3.1.4. Glass Cutting Template
- 3.1.5. Metal Ruler or Metal Putty Knife
- 3.1.6. Silicon Wafer Plastic Storage Container
- 3.1.7. Fluke® Digital Multimeter
- 3.1.8. Kimwipes® Laboratory Tissue Paper
- 3.1.9. Metric Measurement Caliper

3.2. Quantity

- 3.2.1. A total of sixteen glass electrodes will be produced from each 5cmx5cm sheet of glass
- 3.2.2. Glass may be cut all at once to save time, but can also be cut on a weekly schedule

3.3. Procedure

- 3.3.1. It is imperative that the FTO coated glass always be handled extremely careful so that the delicate conductive layer is not scratched
- 3.3.2. To find the conductive side of the glass, use a digital multimeter (DMM) to test for continuity
- 3.3.3. Place a small strip of 3M[®] low tact artist tape on the bottom surface of the template labeled “5cmx5cm Glass Cutting Template” on each of the four corners to protect the conductive FTO surface of the glass





- 3.3.4. Place a 5cmx5cm sheet of glass into the template, conductive side facing down
- 3.3.5. Place the template in the upper left corner of the laser tray



- 3.3.6. Power on the laser (the switch is located on the right side of the laser) then power on the computer
- 3.3.7. Turn on fume-hood exhaust fan and plug-in exhaust pump
- 3.3.8. Set the tray height by pressing the “Z” button on the laser control panel. Use the calibration tool by placing the tool on the template, then press the up or down button to adjust the tray height to align with the grooves on the calibration

tool with the lasers lens housing box. Press the “Z” button when alignment has been realized.



- 3.3.9. Inside the desktop folder titled “DSSC Cutting File,” open the “Glass Cutting” folder and open the CorelDRAW® 12 file named “Glass Horizontal.cdr”
- 3.3.10. Change print settings:
 - 1) Click File
 - 2) Click Print
 - 3) Click Preferences
 - 4) Click Red
 - 5) Ensure the Power = 55%, Speed = 5, PPI = 600
 - 6) Click Set
 - 7) Click OK
 - 8) Click Apply
 - 9) Click Print
- 3.3.11. Press the laser’s “Start” button 
- 3.3.12. Open the CorelDRAW® 12 file named “Glass Vertical.cdr”
- 3.3.13.
 - 1) Click File
 - 2) Click Print
- 3.3.14. Press the laser’s “Start” button 
- 3.3.15. Carefully remove the glass and template from the laser tray and place the glass (FTO layer facing upwards) onto a clean Kimwipe®
- 3.3.16. Discard any unusable glass pieces (ones that are shorter than 12mm on the length or width, or have cracks or chips that would impact performance or assembly efforts)
- 3.3.17. Scrape off the small glass shards from the sides of each piece of glass with a hard but non-abrasive object being extremely careful not to make contact with the glass surface area. Use a metal ruler, metal putty knife or any rigid object.

- 3.3.18. Store the electrodes (FTO layer facing upwards) in the “cut glass” wafer container

4. PREPARING SEALANT

4.1. Materials/Equipment

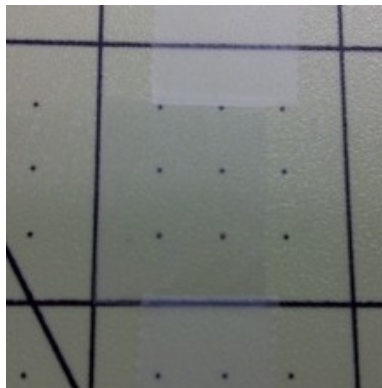
- 4.1.1. Meltonix 1170-60 Hot Melt Sealing Film (60µm thick)
- 4.1.2. Westcott® Paper Trimmer
- 4.1.3. 3M® Scotch® Magic™ Tape
- 4.1.4. C-Thru Square Template
- 4.1.5. X-ACTO® Precision Knife
- 4.1.6. Rubber Cutting Mat
- 4.1.7. Small Storage Container
- 4.1.8. Kimwipes® Laboratory Tissue Paper
- 4.1.9. 100% Pure Ethanol

4.2. Quantity

- 4.2.1. One sealant to bond each solar cell together, totaling four for each week

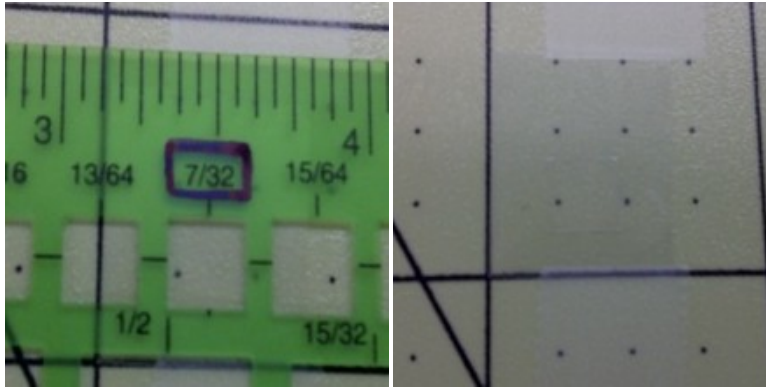
4.3. Procedure

- 4.3.1. Thoroughly clean any lint or dust from all the materials and working area with ethanol and Kimwipes® before beginning the procedure
- 4.3.2. Cut a 15mm strip of Meltonix sealant from the large sealant sheet using the paper trimmer
- 4.3.3. Cut off 15mm segments of the sealant strip using the paper trimmer (this makes 15mmx15mm individual square pieces of sealant)
- 4.3.4. Secure the individual sealant squares onto a cutting mat with Magic™ tape, being careful to contact as little sealant as possible



- 4.3.5. Using the C-thru square template, position the 7/32” square opening as shown below. Hold down the template

firmly to prevent an uneven cut while using the size #17 X-ACTO[®] blade.



- 4.3.6. Position the blade against the inside wall of the template square and press down firmly. Do this for all four square sides. Being extremely careful not to move the template.
- 4.3.7. Repeat steps 4.3.4 - 4.3.6 for all of the 15mmx15mm sealant squares
- 4.3.8. Store the completed sealants in a sealed container for later use

5. DRILLING COUNTER ELECTRODE

5.1. Materials/Equipment

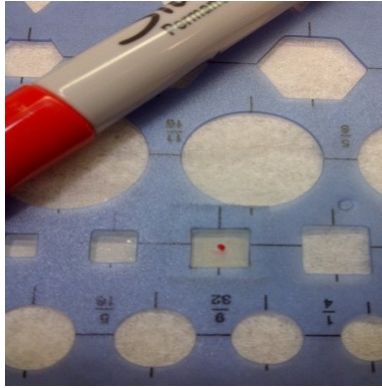
- 5.1.1. #77 (0.018") Solid Carbide Drill Bit
- 5.1.2. (4) 12.5mm x 12.5mm Glass Electrodes
- 5.1.3. High Speed Drill Press
- 5.1.4. Silicon Wafer Plastic Storage Container
- 5.1.5. Permanent Felt CD Marker - Red
- 5.1.6. 100% Pure Ethanol
- 5.1.7. Kimwipes[®] Laboratory Tissue Paper

5.2. Quantity

- 5.2.1. This procedure prepares four drilled counter electrodes. The drilled hole will be the entry point for the electrolyte during the final cell assembly process. These electrodes (glass pieces) are considered to be the counter electrode (CE) component of the solar cell, on which the platinum layer will eventually be deposited onto.

5.3. Procedure

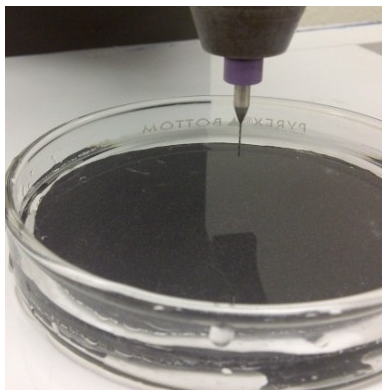
- 5.3.1. Mark a drilling point on the non-conductive side of the glass. This can be performed by using a CD marker to dot the center point of the active area. For help centering the mark, use a square template to visualize the active area.



- 5.3.2. Repeat the previous step for all four electrodes
- 5.3.3. Place a size #77 solid carbide drill bit in the high speed drill press



- 5.3.4. Fill a Petri dish ½ full of water



- 5.3.5. Place one glass electrode, conductive layer facing upwards, into the Petri dish containing water
- 5.3.6. Hold down the glass with the left hand index finger and thumb. Using the right hand, turn the drill press power on.

- 5.3.7. Gently guide the drill down onto the marked target, pressing down slowly. Let the drill bit work its own way through the glass.
- 5.3.8. When the drill bit is nearly 4/5 of the way through the glass, ease up (almost entirely) and let the drill bit finish the final segment of the hole.
 - Important Note – even a small amount of excessive pressure can cause a fairly large blow-out on the non-conductive side of the electrode.
- 5.3.9. Raise the drill by slowly backing off of the drill press crank handle
- 5.3.10. Set aside the drilled electrode, conductive layer facing upwards to prevent damage to the fragile surface
- 5.3.11. Repeat the drilling process (steps 4.3.6 - 4.3.11) for all four electrodes
- 5.3.12. Turn off the drill press, being extremely careful not to allow sleeves, hair or hands to contact the rotating drill bit when reaching across the drill press
- 5.3.13. Gently clean off the marker spot with ethanol and Kimwipes®
- 5.3.14. Store the electrodes in the plastic silicon wafer storage container

6. RUTHENIUM DYE SOLUTION PREPARATION

6.1. Materials/Equipment

- 6.1.1. Ruthenizer 535-bisTBA Dye (aka N719)
- 6.1.2. 100% Pure Ethanol
- 6.1.3. PARAFILM® Wax Paper
- 6.1.4. Permanent Felt CD Marker - Black
- 6.1.5. VWR® 3"x 3" Weighing Paper
- 6.1.6. Kimwipes® Laboratory Tissue Paper
- 6.1.7. Mettler Toledo® Precision Scale
- 6.1.8. (2) Sealing Wide Mouth Jars
- 6.1.9. VWR® Ultra-sonic Stirring Bath

6.2. Quantity

- 6.2.1. Make two jars of dye solution, 20mL per jar
- 6.2.2. The solution is considered "good" until there are noticeable particles of TiO₂ flakes present in the dye solution

6.3. Procedure

- 6.3.1. Wipe out the inside of the jars and the 80mL glass beaker with a Kimwipe® and ethanol.
- 6.3.2. Add 20mL of pure ethanol to each jar
- 6.3.3. Place a single weighing paper on the precision scale, then close the sliding doors

- 6.3.4. Zero the scale by pressing the “O/T” button
- 6.3.5. Measure 6.15mg of Ruthenium dye on the precision scale, ensuring that the sliding doors are closed during the readout
- 6.3.6. Carefully drop 6.15mg of dye into each jar with the 20mL of pure ethanol already present
- 6.3.7. Firmly hand tighten the lid of each jar
- 6.3.8. Place the two jars into the ultra-sonic stirring bath filled with around 2” of water. Set the built-in timer on the stirrer for fifteen minutes, and then press start to begin the ultrasonic stirring process.
- 6.3.9. Remove the jars from the ultra-sonic bath
- 6.3.10. Label each jar with the date that the solution was made.
- 6.3.11. Store the dye solutions in a dark environment to avoid unnecessary evaporation of the ethanol

7. FABRICATING WORKING ELECTRODE

7.1. Materials/Equipment

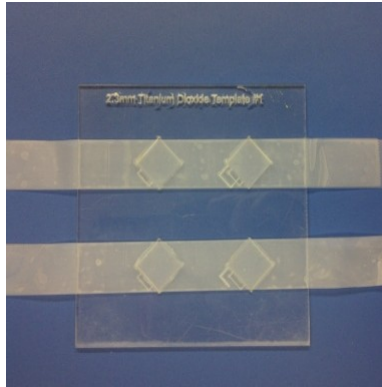
- 7.1.1. Titanium Dioxide Template
- 7.1.2. 3M[®] Scotch[®] Magic[™] Tape
- 7.1.3. Syringe
- 7.1.4. 5cmx5cm Glass Sheet
- 7.1.5. Kimwipes[®] Laboratory Tissue Paper
- 7.1.6. Large Plastic Storage Box
- 7.1.7. Universal Laser System – Laser/Engraver
- 7.1.8. Pyrex[®] Petri Dish Set
- 7.1.9. Barnstead[®] Thermolyne 6000 Furnace
- 7.1.10. Ti-Nanoxide D – Opaque Nanocrystalline Titanium Dioxide Paste
- 7.1.11. Craftsman[®] Spring loaded tweezers

7.2. Quantity

- 7.2.1. Four working electrodes will be fabricated upon completion of this procedure. The working electrodes consist of the 2.2mm FTO coated glass with a 40 μ m thick (area 49mm²) layer of sintered TiO₂.

7.3. Procedure

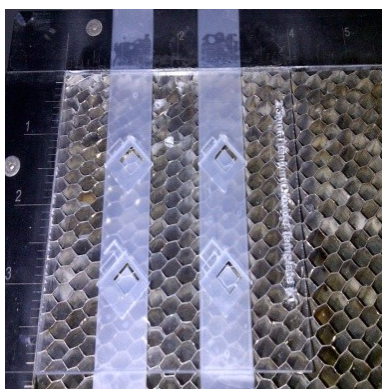
- 7.3.1. Wipe down tools, coating machine and working station with Kimwipes[®] and ethanol
- 7.3.2. Using a TiO₂ template, place a strip of tape (with an extra 1” overhang) from the top to bottom over the two diamond shaped openings parallel to the template title: “2.3mm Titanium Dioxide Template #1”
- 7.3.3. Place two more layers of tape, equaling three, ensuring no large air bubbles exist between the layers



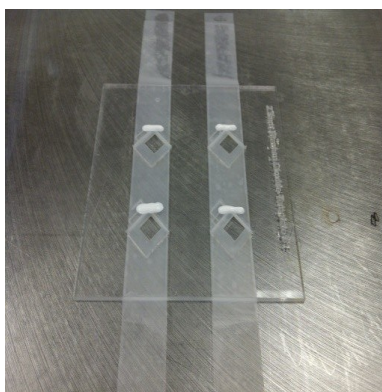
- 7.3.4. Repeat steps 7.3.2 and 7.3.3 on the other two openings of the template
- 7.3.5. Turn on laser and computer
- 7.3.6. Turn on fume-hood exhaust fan and plug-in exhaust pump
- 7.3.7. Insert the template in upper left corner of the laser tray



- 7.3.8. Open file named "TiO₂ active area 2.3mm.cdr"
- 7.3.9. Change the print settings to: Power 35%, Speed 5, and PPI 600 (refer to step 3.3.10)
- 7.3.10. Press the lasers "Start" button
- 7.3.11. Place each template back into a storage container after the active areas have been cut into the tape like the one below



- 7.3.12. Insert a glass electrode into each opening of the templates. Center the glass with an approximate 1mm space left on the flattest side, making sure to have the conductive layer facing up through the cutouts.
- 7.3.13. Add 3 small squares of tape under each glass electrode to build up the height of the electrodes to equal the height of the template.
- 7.3.14. Optional Step: If the TiO_2 paste begins to separate or is unusually thick, stir the paste for five minutes in the ultrasonic stirring bath. Shaking the bottle causes air bubbles to form in the paste, which will negatively impact ability to apply a uniform layer of paste.
- 7.3.15. Using the syringe, deposit an even line of TiO_2 paste directly above the glass electrodes



- 7.3.16. Pull the 5cmx5cm glass sheet at a 45° lagging angle over the paste and electrode. Allow the weight of the glass sheet to determine the applied coating pressure on the tape.
- 7.3.17. Repeat on the remaining three electrodes
- 7.3.18. Partially cover the template with a lid to reduce the likelihood of particulates settling on the wet TiO_2 layer. The

- purpose of a partial opening is to minimize condensation from forming on the TiO₂ solution.
- 7.3.19. Leave the TiO₂ coated electrodes undisturbed for thirty minutes before handling
 - 7.3.20. The layers may be uncovered when the bright white TiO₂ layer fades into a grayish tint. This color change is due to the evaporation of alcohol in the TiO₂ paste.
 - 7.3.21. Remove the tape by slowly pulling at roughly a 30° angle. Be especially careful that nothing touches the TiO₂ layers when removing the tape.
 - 7.3.22. Carefully remove the TiO₂ electrodes and place them in a Petri dish with a lid
 - 7.3.23. Place the Petri dish filled with the freshly coated TiO₂ active electrodes into the furnace
 - 7.3.24. Make sure the ventilation cover and furnace door are closed, and a notification sign is displayed so that the TiO₂ sintering process will not be disturbed
 - 7.3.25. Turn the power on the furnace and set the temperature to 400°C
 - 7.3.26. Begin counting down 1:45:00 minutes with a timer
 - 7.3.27. At the conclusion of 1:45:00, keep the door and vent cover closed, turn the furnace power off and keep the door closed for >12 hours to allow the TiO₂ layer to gradually reach room temperature
 - 7.3.28. Remove the Petri dishes from the furnace and transport to the coating room
 - 7.3.29. Using the spring loaded tweezers, remove the TiO₂ active electrodes from the Petri dish and place into a dye solution jar.
 - 7.3.30. Tightly close the lids of the jars and allow to soak for >12 hours to complete saturation absorption
 - 7.3.31. Leave the TiO₂ to soak in the dye solution until final assembly

8. PREPARING COUNTER ELECTRODE

8.1. Materials/Equipment

- 8.1.1. Platinum Template
- 8.1.2. 3M[®] Scotch[®] Magic[™] Tape
- 8.1.3. Pyrex[®] Petri Dish Set
- 8.1.4. Platinum Catalyst Paint - Platisol T/SP
- 8.1.5. Disposable Liquid Dropper
- 8.1.6. Plastic Squeegee
- 8.1.7. 100% Pure Ethanol
- 8.1.8. Kimwipes[®] Laboratory Tissue Paper

- 8.1.9. Barnstead® Thermolyne 6000 Furnace
- 8.1.10. Silicon Wafer Plastic Storage Container
- 8.1.11. Universal Laser Systems - Laser/Engraver

8.2. Quantity

- 8.2.1. Four platinum nano-particle coated counter electrodes will be prepared following this procedure

8.3. Procedure


- 8.3.1. Clean a work station, equipment, and four drilled electrodes using Kimwipes® and ethanol
- 8.3.2. Place a long strip of magic tape over four square openings of the platinum template
- 8.3.3. Place a second layer of tape over the first layer, being careful not to allow large air bubbles between the layers. If large air bubbles are present, discard the tape layer and try again. Use your finger to smooth out the layers.



- 8.3.4. Place the platinum template in the upper left corner of the laser tray and close the laser cover

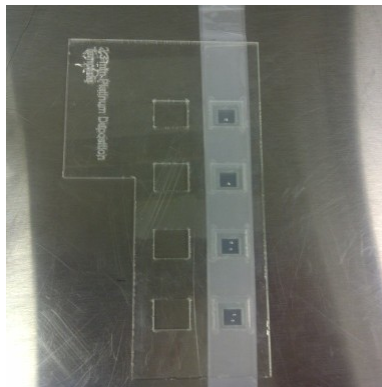


- 8.3.5. Turn on the laser and computer
- 8.3.6. Turn on fume-hood exhaust fan and plug-in exhaust pump

- 8.3.7. Ensure the laser tray is aligned to the correct height (refer to step 3.3.8)
- 8.3.8. Open the file named "Platinum active area 2.3mm.cdr"
- 8.3.9. Change the print settings to: Power 35%, Speed 5, and PPI 604 (refer to step 3.3.9)
- 8.3.10. Press the laser's "Start" button 
- 8.3.11. The templates should now look similar to the image below



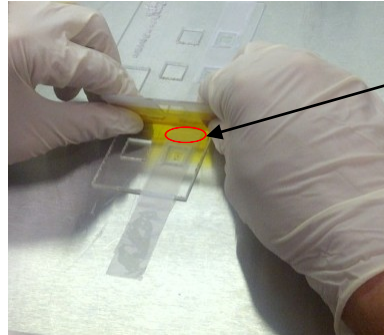
- 8.3.12. When finished cutting the active areas - turn off the laser, computer, fume-hood and unplug the power cord for the exhaust fan
- 8.3.13. Next, insert a drilled counter electrode into the back side of the template, ensuring the conductive layer faces the tape. Also check to make sure that a 1mm space is left between the bottom of the glass and the opening of the square.



- 8.3.14. Use your gloved finger or a non-abrasive tool, press the tape firmly on the glass to ensuring a proper seal is made between the glass electrode and the tape
- 8.3.15. Using a disposable dropper, deposit two small drops of Platisol directly above the glass to be coated. The liquid is inviscid so it will spread quite quickly, but the initial

diameter of the drop should be roughly the diameter of a pea.

- 8.3.16. Drag the Platisol with a squeegee at a 60° angle over the glass



Deposit the Platisol drops above the template openings as indicated in the picture

- 8.3.17. Upon total evaporation of the Platisol, apply one more layer by repeating steps 8.3.15 - 8.3.16 to each electrode (each electrode should have a total of two layers when completed)
- 8.3.18. Put the lid tightly back on the bottle of Platisol
- 8.3.19. Cover the template and allow the Platisol liquid to dry for five minutes
- 8.3.20. Remove the tape from the template
- 8.3.21. Place all the freshly coated counter electrodes in one clean Petri dish with a lid
- 8.3.22. First making sure the furnace is near room temperature; place the Petri dish inside the furnace
- 8.3.23. Close the furnace door
- 8.3.24. Turn the furnace to "On" and set the adjustable thermostat to 400°C
- 8.3.25. Make sure the furnace door and top lid are closed
- 8.3.26. Set a timer for 1:45:00
- 8.3.27. Attach a sign to notify others that the furnace is in use for the next 14 hours
- 8.3.28. Turn the power off when the timer signals the sintering process has been completed. Make sure to leave the furnace door closed and undisturbed for an additional 12 hours.
- 8.3.29. Remove the Petri dishes from the furnace and store the entire Petri dish with included contents in a plastic sealed silicon wafer storage container
- 8.3.30. The platinum electrodes must be used in assembly within 24 hours or they must be reheated in the furnace at 400°C for 15 minutes to reactivate the nano-particles

9. ASSEMBLING SOLAR CELL

9.1. Materials/Equipment

- 9.1.1. Kimwipes[®] Laboratory Tissue Paper
- 9.1.2. Pyrex[®] Petri Dish Set
- 9.1.3. 100% Pure Ethanol
- 9.1.4. Westcott[®] Paper Trimmer
- 9.1.5. Kapton[®] High Temperature Tape
- 9.1.6. Hot Glue Gun with Hot Glue Stick
- 9.1.7. (4) Precut Meltonix Sealant Melts (Section 4)
- 9.1.8. (4) Prepared Titanium Dioxide Layered Active Electrodes (Section 7)
- 9.1.9. (4) Prepared Platinum Layered Counter Electrodes (Section 8)
- 9.1.10. Solaronix[®] AN-50 Electrolyte
- 9.1.11. Solaronix[®] Vacuum Needle
- 9.1.12. Permanent Felt CD Marker
- 9.1.13. Hotplate
- 9.1.14. Hex Nut Driver
- 9.1.15. Precision Tweezers
- 9.1.16. Craftsman[®] Spring Loaded Soft Tip Tweezers

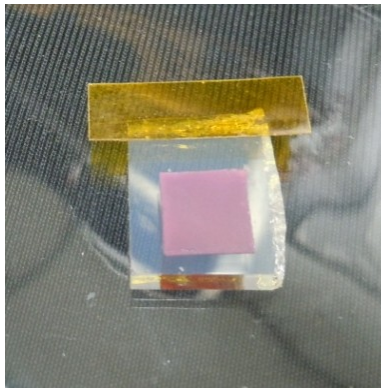
9.2. Quantity

- 9.2.1. This procedure is the final fabrication step which places four counter electrodes together with four active electrodes, for a total of four completed dye-sensitized solar cells

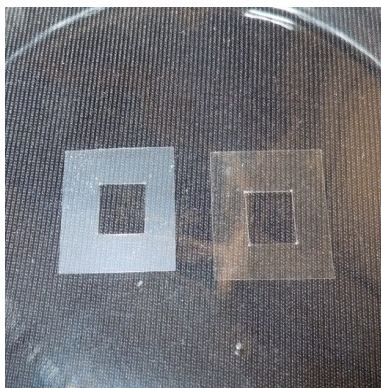
9.3. Procedure Instructions

- 9.3.1. Begin by cleaning a work space and the equipment with Kimwipes[®] and ethanol, with the exception of the platinum and titanium dioxide electrodes
- 9.3.2. In preparation for later steps, turn on the hotplate and set it to 110°C
- 9.3.3. Remove the TiO₂ electrodes from the dye solution. Place in a Petri dish with the active layer facing upwards to avoid damaging the titanium dioxide. It is very important that you maintain the order of each set of four electrodes for classification.
- 9.3.4. Gently spray the excess dye off of the glass with ethanol. Use a separate Petri dish to temporarily store the rinsed off electrodes.
- 9.3.5. Allow the ethanol a few minutes to dry from the TiO₂ electrodes before handling
- 9.3.6. Cut off 2-3mm strips of kapton tape from the roll using the paper trimmer. You will need twelve strips for the four cells.

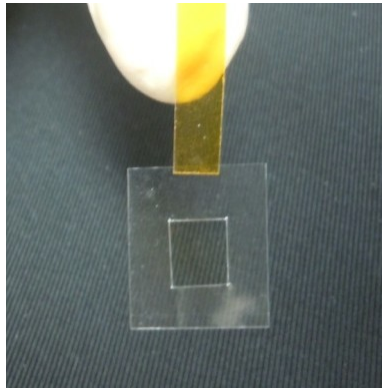
- 9.3.7. Place an individual TiO_2 electrode face-up onto the center of an upside down clean Petri dish lid
- 9.3.8. Protect a strip of conductive FTO layer by placing a single piece of Kapton[®] tape on the edge of the active electrode. This will keep the sealant from melting onto the area of the electrode that will later contact the testing leads.



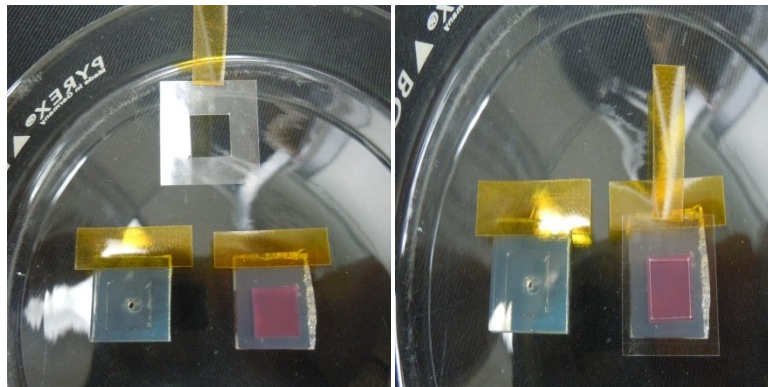
- 9.3.9. Take a pre-cut sealant and remove the protective film, which has a blue tint



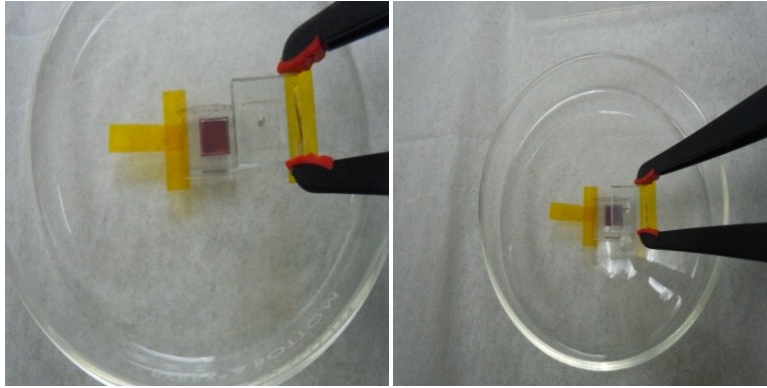
- 9.3.10. Place a piece of Kapton[®] tape at the middle end of the shorter side of the sealant



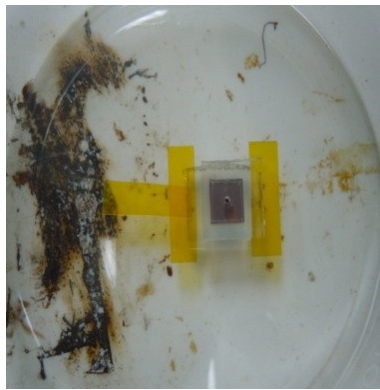
- 9.3.11. Using a pair of precision tweezers, place a single sealant (Kapton[®] tape facing downward) carefully over the TiO₂; make sure that the sealant opening is centered almost perfectly over the TiO₂ layer. This step takes quite a bit of practice because static electricity along with the slightest movements will create drastic misalignments between the layers.



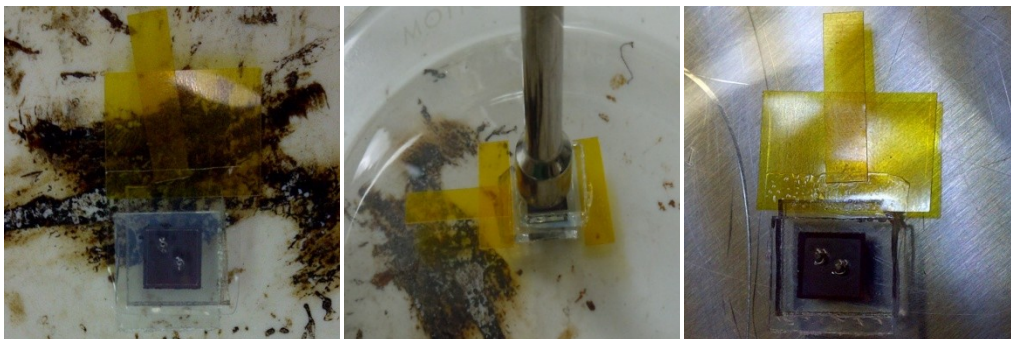
- 9.3.12. Once the sealant is aligned, press the Kapton[®] tapes together with tweezers to adhere the sealant and TiO₂ electrode together.
- 9.3.13. Using the spring loaded soft tipped tweezers, place a platinum electrode face-down over the sealant, ensuring the glass electrodes do not overlap the Kapton[®] tape, but yet the active areas align. The active area of the platinum layer will be visible by looking through the top of each counter electrode. If unsure which side is conductively coated, use a digital multimeter on the audible impedance setting to identify the conductive layer. Simple mistakes such as mixing the sides of the platinum will ruin the entire cell and costing valuable resources.



9.3.14. Carefully pick-up the Petri dish containing the assembled cell and place it on the center of the hot plate.



9.3.15. Leave the cell on the hotplate for two and a half to three minutes, watching closely to see when the sealant turns from a grayish color into a more opaque/clear color. As soon as you notice that most of the sealant has turned clear, use a hex nut driver to apply pressure to the top of the cell for ten seconds to get an even bond with the glass and press the remaining bubbles out of the sealant.



- 9.3.16. Remove the Petri dish from the hotplate. Set aside, being careful to maintain proper order of the four cells.
- 9.3.17. Filling the assembled cells with electrolyte is the next step.
- 9.3.18. Plug-in the power cord of the hot glue gun and set aside.
- 9.3.19. Remove a few milliliters (mL), or about a half inch in the syringe vial, of electrolyte from the bottle of AN-50 electrolyte using the vacuum needle. Purge the air from the needle by holding the needle upside down and compressing the needles chamber until all that remains in the vacuum needle is electrolyte. Place the opening of the needle over the drill hole of one of the cells and release the pressure from the needle. This will purge the air from the cell. Gently inject the electrolyte into the hole until the electrolyte has filled the entire cavity and drill hole.
- 9.3.20. Remove the needle from the cell and wipe off the electrolyte from the top (drilled electrode side) of the cell. Clean the electrolyte from the outside of the cell with a Kimwipe[®], using ethanol to clean off the electrolyte that may not be visible. Hot glue will not bond to glass that is not entirely dry and clean.
- 9.3.21. Seal the drilled hole by depositing a pea sized drop of hot glue directly over the opening of the hole
- 9.3.22. Clean the rest of the cell with a Kimwipe[®]
- 9.3.23. Mark the cell with an identification number and letter using a permanent CD marker



- 9.3.24. Repeat steps 9.3.22 - 9.3.26 until all the cells have been entirely assembled and labeled
- 9.3.25. Store the cells in a small labeled plastic box. The cells are now complete and will be ready for performance measurements in 1-2 days.



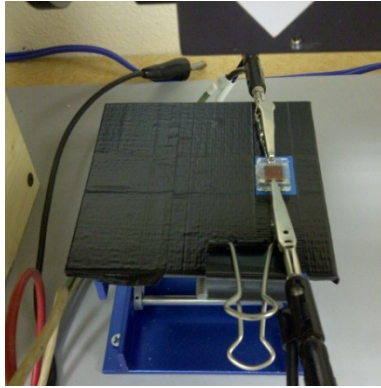
10. PERFORMANCE MEASUREMENTS / DATA COLLECTION

10.1. Materials

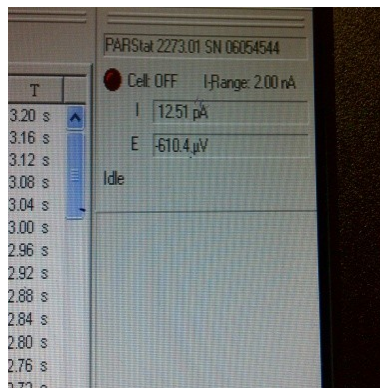
- 10.1.1. Parstat[®] Electrochemical Machine
- 10.1.2. Dell[®] Desktop Computer
- 10.1.3. Digital Thermometer with a Thermocouple
- 10.1.4. Newport[®] “Class C” Solar Simulator
- 10.1.5. Adjustable Platform
- 10.1.6. Fan
- 10.1.7. Kimwipe[®] Laboratory Tissue Paper

10.2. Procedure

- 10.2.1. Power on the computer, solar simulator, electrochemical machine and fan
- 10.2.2. Press “Cell Enable,” located on the front control panel of the Parstat[®] electrochemical machine
- 10.2.3. Place a cell to be measured over the marked target of the platform
- 10.2.4. Attach the black/gray leads of the electrochemical machine to the active electrode (cell electrode without the hole) using an alligator clip
- 10.2.5. Secure the red/white leads with the attached alligator clip to the platform with a binder clip
- 10.2.6. Press open the alligator clip attached to the platform. Position the counter electrode (bottom electrode with the drilled hole) between the alligator clips’ teeth and release the alligator clip to secure the electrode.
- 10.2.7. The solar cell should now be properly positioned for data collection measurements.

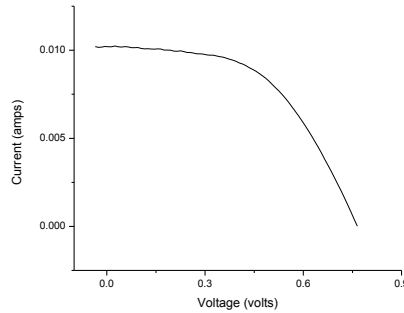


- 10.2.8. Open the Powersuite[®] software on the computer desktop
- 10.2.9. Locate the correct testing file by opening:
 - 1) Experiment
 - 2) Open
 - 3) PowerCorr
 - 4) Brian DSC Cell Test
 - 5) Select
- 10.2.10. The test is ready after it has completed buffering to 100% and shows “Idle”



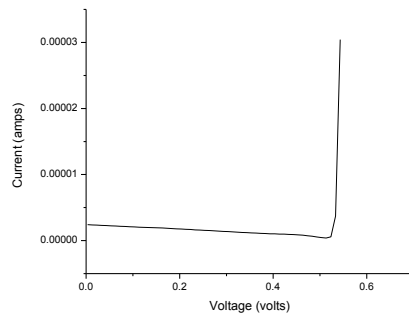
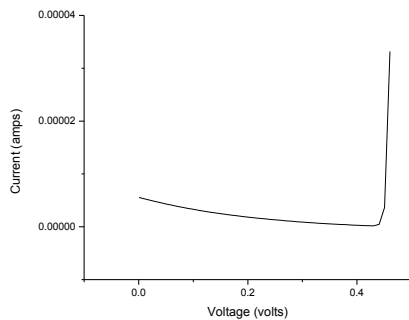
- 10.2.11. Turn on the solar simulators light by pressing the “Lamp Start” button
 - 10.2.12. Press the play button in Powersuite[®] to begin the test
 - 10.2.13. After the curve is completed, right-click anywhere on the plot area. Click “copy data” and paste the raw data into a Microsoft[®] Excel document to record the data
 - 10.2.14. To find the efficiency, paste the raw data into the 1st cell of the Excel document labeled “2.3mm DSC Spreadsheet” to find the cell efficiency
- 10.3.I-V Curve Interpretations**
- 10.3.1. *Ideal Curve* – A square shape indicates that the solar cell has been properly constructed and all the major

mechanisms are functioning correctly with little internal resistance losses.



10.3.2. *Exponentially Decreasing Curve* – You can expect to see a similar curve when the supply of electrolyte has evaporated and is nearly depleted. This is often caused from improper sealing, but regardless of the sealing, will occur naturally over time due to the unavoidable tendency of liquids to evaporate. The sharply decreasing line depicts a near open circuit condition, meaning that there is minimal to no connection between the anode and cathode (electrodes).

If electrolyte can be seen in the drilled cavity on the counter electrode, then check to make sure that the cables are properly connected from the Parstat[®] machine to the tested solar cells' electrodes. Run the performance test again to see if that resolved the issue. If the same condition still persists, check to see if there is overhanging sealant between the alligator clips and the electrodes, or that the conductive layers are facing the correct direction.



10.3.3. *Linear Curve* – This line represents a short circuit within the cell. If the sealant fails to contain the electrolyte within

the active area, there will be a shorting between the conductive layers of the two electrodes. A large leak will look like the image below. Smaller leaks or misaligned sealants can still be observed but will be less obvious.

